Multidimensional mapping of root responses to soil environmental cues using a luminescence-based imaging system

Rubén Rellán-Álvarez[1, 9], Guillaume Lobet[2], Heike Lindner[1, 8], Pierre-Luc Pradier[1, 8, 10], Muh-Ching Yee[1], Jose Sebastian[1], Yu Geng[1, 7], Charlotte Trontin[1], Therese LaRue[3], Amanda Schrager-Lavelle[4], Cara Haney[5], Rita Nieu[6], Julin Maloof[4], John P. Vogel[7], José R. Dinneny[1, 12]

[1] Department of Plant Biology, Carnegie Institution for Science, Stanford, CA, USA.

[2] PhytoSystems, University of Liège, Liège, Belgium.

[3] Department of Biology, Stanford University, Stanford, CA, USA.

[4] Department of Plant Biology, UC Davis, Davis, CA, USA.

[5] Harvard Medical School/Massachusetts General Hospital, Department of Genetics/Department of Molecular Biology Boston, MA, USA

[6] USDA Western Regional Research Center, Albany, CA, USA

[7] DOE Joint Genome Institute, Walnut Creek, CA, USA

[8] These authors contributed equally

[9] Present address: Unidad de Genómica Avanzada (Langebio), CINVESTAV, Irapuato, México.

[10] Present address: Boyce Thompson Institute for Plant Research/USDA, Ithaca, NY, USA.

[11] Present address: Energy Biosciences Institute, UC, Berkeley, CA, USA

[12] Corresponding author

Author contributions:

RR-A: Conception, design and development of the growth and imaging system and Arabidopsis transgenic lines; acquisition, analysis and interpretation of data; drafting and revising the article.

GL: Development of the GLO-RIA image analysis plugin, analysis and interpretation of data, drafting and revising the article.

HL: Acquisition of data, development of the tomato growth and imaging setup.

P-LP: Acquisition of data, analysis and interpretation of data

MCY: Development of Arabidopsis and Brachypodium transgenic lines.

JS: Development of Brachypodium transgenic lines, acquisition and analysis of Brachypodium data.

YG: Development of Arabidopsis transgenic lines.

CT: Acquisition and analysis of the QPCR data

TL: Acquisition and analysis of the QPCR data

AS-L: Contributed the unpublished dual-color tomato line.

CH: Contributed the unpublished *Pseudomonas fluorescens* CH267-lux strain.

RN: Contribution to the development of the Brachypodium transgenic line.

JM: Contributed the unpublished dual-color tomato line.

JPV: Contribution to the development of the Brachypodium transgenic line.

JRD: Conception, design and development of the growth and imaging system and Arabidopsis transgenic lines; acquisition, analysis and interpretation of data; drafting and revising the article.

All authors read and approve the final version of the manuscript.

Abstract

Root systems develop different root types that individually sense cues from their local environment and integrate them with systemic signals. This complex multi-dimensional amalgam of inputs leads to continuous adjustment of root growth rates, direction and metabolic activity to define a dynamic physical network. Current methods for analyzing root biology balance physiological relevance with imaging capability. To bridge this divide, we developed an integrated imaging system called Growth and Luminescence Observatory for Roots (GLO-Roots) that uses luminescence-based reporters to enable studies of root architecture and gene expression patterns in soil-grown, light-shielded roots. We have developed image analysis algorithms that allow the spatial integration of soil properties such as soil moisture with root traits. We propose GLO-Roots as a system that has great utility in both presenting environmental stimuli to roots in ways that evoke natural adaptive responses, and in providing tools for developing a multi-dimensional understanding of such processes.

Introduction

Plant roots are three-dimensional assemblies of cells that coordinately monitor and acclimate to soil environmental change by altering physiological and developmental processes through cell-type and organ-specific regulatory mechanisms[1,2]. Soil comprises a complex distribution of particles of different size, composition and physical properties, airspaces, variation in nutrient availability and microbial diversity[3,4]. These physical, chemical and biological properties of soil can vary on spatial scales of meters to microns, and on temporal scales ranging from seasonal change to seconds. Root tips likely monitor this environment through locally and systemically acting sensory mechanisms[5,6].

The architecture of the root system determines the volume of soil where resources can be accessed by the plant (rhizosphere). Because the physical and chemical properties of these resources vary, their distribution in the soil column is distinct[4]. Water and water-soluble nutrients such as nitrogen or manganese move through the soil by bulk flow and

tend to accumulate deeper in the soil profile as a consequence of gravity[7], while other nutrients such as phosphorus and potassium, which tightly bind to soil particles, tend to accumulate in the upper layers of soil where decomposition of organic matter replenishes their supply[7]. Developmental processes that affect root growth rate and direction will influence the efficiency with which specific resources are captured from the rhizosphere. Root systems optimized to capture one resource may be inefficient for another.

Root architecture is under both environmental and genetic control; plasticity in growth parameters allows the plant to adjust its form to suit a particular soil. Lateral roots, which usually make up the majority of the total root system, often grow at an angle divergent from the gravity vector. This gravity set-point angle (GSA) is controlled by auxin biosynthesis and signaling and can be regulated by developmental age and root type[8]. Recent cloning of the *DRO1* Quantitative Trait Locus (QTL) demonstrates that natural genetic variation is a powerful tool for uncovering such control mechanisms[9].

Specific root ideotypes (idealized phenotypes) have been proposed to be optimal for acquisition of water and nitrogen, which are distinct from ideotypes for low phosphorus. Based on computational modeling and field studies, the "steep, deep and cheap" ideotype proposed by Lynch and colleagues may provide advantages to the plant for capturing water and nitrogen. This ideotype consists of highly gravitropic, vertically oriented roots that grow deep in the soil column and develop large amounts of aerenchyma, which reduces the overall metabolic cost of the root system[3]. Low phosphorus conditions, on the other hand, favor roots systems that are more highly branched and shallow. Modeling of root system variables shows that optimum architecture for nitrogen and phosphorus uptake are not the same[10] and suggests tradeoffs that may affect the evolution of root architecture as a population adapts to a particular environmental niche.

Clearly understanding the architecture of root systems and how environmental conditions alter root developmental programs is important for understanding adaptive mechanisms of plants and for identifying the molecular-genetic basis for different response programs. Experimental methods for studying root architecture can be divided into two general categories

that each represent compromises in either physiological relevance or versatility.

Growth of plants in gels such as agar or gellan gum provides a transparent support medium which allows immediate visual access to roots. Simple devices can be used to capture macroscopic images of roots[11] or confocal microscopy can be implemented for studying cell-scale processes. Gel-media allows exact control over the concentration of nutrients[12] or stressful components[13] and fluorescent reporters can be deployed to track the activity of genes, proteins or metabolites. This approach has been extensively used in the model plant Arabidopsis and has allowed for the discovery of many fundamental processes. Root system architecture studies and high resolution time-scale analysis of root growth are easily performed when used in combination with automatic time-lapse imaging[14,15]. Variations of this approach have been used in other species to study root system architecture in three dimensions[17]. Most often, in gel-based media systems, roots are exposed to light[18] while shoots are enclosed in a high-humidity head-space that does not permit transpiration from the leaf surface. Media is typically axenic and with highly artificial levels and distributions of nutrients. Gas exchange between the root and the media is limited and might lead to hypoxia or ethylene buildup. *In vitro* growth conditions are also limited in the length of time plant growth can be supported. Typical studies examine roots during the first 1-2 weeks after seed germination whereas the life-cycle of Arabidopsis lasts for two months or longer, depending on the accession. Morevover, the relevance of root architectural phenotypes that are highly influenced by light raises concerns regarding the importance of any loci identified using in vitro conditions[18]. Due to these limitations, studying processes that involve whole-plant sensing of environmental cues such as water or nutrient availability must be viewed with caution.

A less transparent but more physiologically relevant medium to study root growth is soil. Plants are grown in soil in the field or in pots. Root imaging can be achieved by several means, from uprooting plants using a shovelomics pipeline[19,20] to growth of roots in transparent pots or in rhizotrons[21], literally "root devices" that are constructed to allow visualization of roots in proximity to a transparent glass or plastic plate. More recently, the

use of techniques such as X-ray micro computed tomography has opened the possibility of *in situ* characterization of root architecture, water content and soil particles in 3-D[5,22]. Such methods are limited due to their relative cost, the volume of soil that can be imaged, the current limit in resolution and the inability to monitor gene expression or other molecular processes.

Roots systems have additional complexity beyond their architecture that needs to be incorporated into our understanding of plant-environment interactions. Primary and lateral roots exhibit different stress response programs in Arabidopsis[2] and may play specialized roles in water and nutrient uptake. Thus, it is important to develop methods that allow for a multidimensional characterization of the root system that includes growth, signaling, and interactions with other organisms.

Based on these considerations we have developed a new root imaging platform, Growth and Luminescence Observatory for Roots (GLO-Roots), which allows root architecture and gene expression to be studied in soil-grown plants. GLO-Roots is an integrated system composed of custom growth vessels, luminescent reporters and imaging systems. We use rhizotrons that have soil volumes equivalent to small pots and support growth of Arabidopsis from germination to senescence. To visualize roots, we designed plant-codon optimized luciferase reporters that emit light of different wavelengths. To visualize reporter expression, plants are watered with a dilute luciferin solution and imaged afterwards. We have designed a custom luminescence imaging system that automatically captures images of rhizotrons held vertically. The signal from each reporter is distinguished using band-pass filters held in a motorized filter wheel, which enables automated acquisition of images from plants expressing both structural and environmentally and developmentally responsive reporters. We have also developed GLO-RIA (GLO-Roots Image Analysis) software that allows for automated determination of root system area, convex hull, depth, width and directionality, which quantifies the angle of root segments with respect to gravity. GLO-RIA is also able to relate root system parameters to local root-associated variables such as reporter expression intensity or soil-moisture content.

Overall GLO-Roots has great utility in presenting environmental stimuli to roots in physiologically relevant ways and provides tools for characterizing responses to such stimuli at the molecular level whole roots of adult plants over broad time scales.

Results

We have developed an integrated platform for growing, imaging and analyzing root growth that provides advances in physiological relevance and retains the ability to visualize aspects of root biology beyond structure.

THE GLO-ROOTS PLATFORM

GLO-Roots is comprised of four parts: i) growth vessels called rhizotrons that allow plant growth and root imaging; ii) luminescent reporters that allow various aspects of root biology to be tracked in living plants; iii) luminescence imaging system designed to automatically image rhizotrons; iv) GLO-RIA, an image analysis suite designed to quantify root systems imaged using GLO-Roots.

Plant growth system GLO-Roots utilizes custom designed growth vessels classically known as rhizotrons, which hold a thin volume of soil between two sheets of polycarbonate plastic. Acrylic spacers provide a 2-mm space in which standard peat-based potting mix is added. Black vinyl sheets protect roots from light and rubber U-channels clamp the rhizotron materials together. Plastic racks hold the rhizotrons vertically and further protect the roots from light. Rhizotrons and rack are placed in a black tub and about 2 cm of water are added to the bottom to maintain moisture in the rhizotrons during plant growth. The volume of soil in the rhizotrons (100 cm^3) is similar to small pots commonly used for Arabidopsis growth and supports growth of Arabidopsis throughout its entire life cycle (Fig 1A-C and Supplement 1).

While the 2 mm depth of the soil sheet is 20 times the average diameter of the Arabidopsis root tip (approximately 100 microns), we wanted to evaluate whether rhizotron-grown plants

exhibited any obvious stress as a consequence of physical constriction. We compared traits of plants growing in vessels that hold similar volumes of soil but in different geometric shapes. No significant differences in shoot area were observed between the three systems (not shown). The number of lateral roots was significantly lower in pot and cylinder-grown plants compared to rhizotron-grown plants (Fig 1F) whereas primary root length of rhizotron and cylinder-grown plants was similar and significantly greater than for pot-grown plants (Fig 1G) . Thus, these data do not support the hypothesis that rhizotron-grown plants experience physical constriction greater than other vessels holding the same volume of soil.

We next compared root systems grown on the surface of agar or in soil. Shoot weight and primary root length were significantly reduced for gel-grown plants compared to rhizotron- or pot-grown plants suggesting significant differences in the biology of plants grown under these conditions (Fig 1H-I). To determine how soil-grown and gel-grown root systems might differ in their biology, we utilized high-throughput qRT-PCR to study a panel of 77 genes curated from the literature that belong to a wide array of biological pathways including nutrient acquisition and hormone and light response to abiotic stress. Whole roots and shoot samples were collected at the end of the light and dark cycles (16 hour light, 8 hours dark) from plants grown in rhizotrons, pots, and petri dishes with two different media recipes (1X MS, 1% sucrose or 0.25X MS, no sucrose). Principal component analysis of the gene expression values showed a clear separation of soil and gel-grown root systems in the first two principal components with a clear overlap between rhizotron and pot-grown root system samples (Fig 1D). Significant differences in genes associated with flavonoid biosynthesis (*FLAVINOL SYNTHASE1, FLS1*) and phosphorus nutrition (*LOW PHOSPHATE RESPONSE1*, *LPR1, PHOSPHATE STARVATION RESPONSE1, PHR1*) were observed (Fig 1E) Flavonoids contribute to anthocyanin biosynthesis, which are UV-protectants. Importantly, however, flavonoids have also been implicated in the regulation of root developmental traits[23], suggesting that light-induction of these pathways in gel-grown roots could influence such processes. *SUPER ROOT1* (*SUR1*), which promotes biosynthesis of the anti-microbial metabolite indole-glucosinolate, was significantly associated with soil-grown roots, suggesting the non-sterile soil environment may induce genes associated

with defense. *XYLOGLUCAN ENDOTRANSGLUCOSYLASE/HYDROLASE17* (*XTH17*) and TOUCH4 (*TCH4*), both of which respond to touch stimuli, were expressed more highly in soil-grown roots consistent with the presence of physical barriers in soil while growth in gel may present fewer obstructions. Interestingly, shoot samples where not clearly distinguished by growth media and, instead, time of day had a greater effect (Fig. 1E and Figure 1 Supplement 1). These data suggest root systems may be particularly sensitive to media conditions.

Generation of transgenic plants expressing different luciferases Arabidopsis roots cannot be easily distinguished from soil using brightfield imaging due to their thinness and translucency; thus, reporter genes are needed to enhance the contrast between the root and their environment. Luciferase is an ideal reporter to visualize roots: 1) unlike fluorescent reporters, luciferase does not require high-intensity excitation light, which could influence root growth, 2) peat-based soil exhibits no autoluminescence but does autofluoresce at certain excitation wavelengths similar to GFP (data not shown), 3) while GFP is very stable and thus not as suitable for imaging dynamic transcriptional events, the luciferase enzyme is inactivated after catabolism of luciferin, making it ideal for studying processes such as environmental responses. A considerable number of luciferases have been developed that emit light spanning different regions of the visible spectrum, but their utilization has been limited to studies in animals (Table 1).

To determine the efficacy of using luciferase to visualize roots in soil, we codon optimized sequences of *PpyRe8*, *CBGRed*, *LUC2*, and *CBG99* for Arabidopsis expression. In addition, nanoLUC and venus-LUC2[24] were utilized. Constitutive luciferase expression was driven in plants using the *UBQ10* or *ACT2* promoter using vectors assembled through a Golden Gate cloning system[25]. Plants homozygous for a single locus T-DNA insertion were evaluated for in vivo emission spectra and luminescence intensity (Fig 2A). All the evaluated luciferases use D-luciferin as a substrate facilitating the simultaneous imaging of different luciferases except nanoLUC, which uses a proprietary substrate. In general, luciferases with red-shifted emission spectra were less intense than the green-shifted luciferases (Fig 2A). LUC2o showed

an emission maximum at 580 nm and a minor peak at 620 nm while CBG99o lacks the minor peak.

GLO1: a semi-automated luminescence imaging system for rhizotrons Luminescence imaging systems commercially available for biomedical research are usually optimized for imaging horizontally held specimens or samples in microtiter plates. Placing rhizotrons in this position would induce a gravitropic response in plants. Working with Bioimaging Solutions (San Diego, CA) we designed and built a luminescence imaging system optimized for rhizotron-grown plants. GLO1 (Growth and Luminescence Observatory 1) uses two back-thinned CCD cameras (Princeton Instruments, USA) to capture partially-overlapping images of rhizotrons while a motorized stage automatically rotates the rhizotron to capture images of both sides (Fig 2B). A composite image is generated from the images of each side; Fig 2C shows that approximately half of the root system is revealed on each side with few roots being visible on both sides. This result suggests that the depth of soil in the rhizotron is sufficient to block visibility of roots beyond the mid-point of the soil sheet but not so thick that a continuous root system is difficult to reconstruct. We tested the ability of GLO1-generated images to reveal complete root systems by manually quantifying the number of lateral roots in root systems of 8 different plants and testing these results against estimates of lateral root number from images visually inspected by 4 different persons. These comparisons revealed good correlation ((R^2= 0.974)) between actual lateral root counts and image-based estimation, indicating GLO1-generated root images provide an accurate representation of the in soil- root system.

Continuous addition of luciferin did not have any significant effect on shoot weight or primary root length (Figure 2 Supplement 1). After luciferin addition, luminescence signal could be reliably detected in root systems for up to 10 days, depending on the developmental state of the plant.

GLO-RIA: GLO-Roots Image Analysis Current image analysis algorithms are optimized for roots that are continuously visible, since they are designed to work with images

of roots grown in transparent media or on paper. Root systems visualized with GLO-Roots, however, often contain breaks in the continuity of primary and lateral root signal, which likely results from soil particles obscuring the object. We developed a set of image analysis algorithms that were well suited for the complex root systems which GLO-Roots is able to capture. GLO-RIA (Growth and Luminescence Observatory Root Image Analysis) is an ImageJ plugin that can automatically identify the perimeter of the root system and quantify aspects of root system geometry derived from this outline. We have also used a directionality algorithm that utilizes a sobel filter to identify edges in an image and quantifies the proportion of quadrants that exhibit a bias in angle of such edges with respect to the axes of the image. Similar algorithms have been used to quantify dynamic changes in the plant cytoskeleton[26]. Directionality measurements can rapidly capture lateral root angles at the whole root system level without the need to define individual roots.

Continuous imaging of root growth

The size of our rhizotrons enables undisturbed root system development (before roots reach the sides or the bottom of the rhizotron) for about 21-23 days for the Col-0 accession growing under long day conditions; however root traits besides width and depth can continue to be observed until senescence of the plant. An example of a time series spanning 11 to 21 days after sowing (DAS) of Col-0 roots expressing *ProUBQ10:LUC2o* is shown in Fig 3A and Video 1 with a color-coded time projection shown in Fig 3B. Directionality analysis (Fig 3C) shows a progressive change in root system angles from 0 º (vertical) to 45 º as lateral roots take over as the predominant root type. Figure 3D shows the evolution over time of several root traits that can be automatically captured by GLO-RIA (depth, width, area) and others that can be manually quantified (primary root growth rate or number of lateral roots per primary root length.

Root system architecture of different Arabidopsis accessions.

The study of natural variation for root system architecture and root traits is a powerful approach for understanding adaptive strategies plants use to cope with environmental change and for identifying the genetic basis for such differences. In Arabidopsis, Quantitative Trait Locus (QTL) and Genome-Wide Association Studies (GWAS) have led to the identification of genes affecting root development[27]. However, traits are usually measured in seedlings less than 2 week old. Selective pressures that affect allele frequencies in a population likely act on genes that affect root system traits at later stages of the plant life cycle, as well. As a proof of concept to estimate the utility of our root imaging system to phenotype adult root system traits, we transformed a small set of accessions with the *ProUBQ10:LUC2o* reporter and quantified RSA at 22 DAS (days after sowing). GLO-RIA analysis of these root systems identified several root traits that distinguish Col-0, Bay-0 and Sha (Fig 4). Bay-0 shows the deepest and narrowest root system leading to the highest depth/width ratio while Sha has the widest root system. Directionality analysis revealed an abundance of steep-angle regions in the root system of Bay while Sha showed an abundance of shallow-angled regions and Col-0 was intermediate (Fig 4D). Broad sense heritability values for depth (96.3), area (92.0), depth/width (97.8), width (95.7) and vertical center of mass (95.0) were all higher than 90%.

GLO-Roots for Brachypodium and Tomato

To examine the general applicability of the GLO-Roots system for other species we introduced LUC2o-expressing reporters into the model grass *Brachypodium distachyon* and the crop plant *Lycopersicon esculentum* (tomato). Brachypodium is well suited to the GLO-Root system because, like Arabidopsis, its small size allows mature root systems to be studied in relatively small soil volumes[28,29]. *LUC2o* driven by the *ZmUb1* promoter was introduced into Brachypodium using the pANIC vector[30]. Brachypodium roots showed a distinct architecture from Arabidopsis marked by prolific development of secondary and tertiary lateral roots (Fig 5A). This is consistent with other studies that show that Brachypodium has a

typical grass root system[29]. After 26-28 days of growth, shoot-derived crown roots initiated and took over as the predominant part of the root system (not shown). Comparison of root system development in rhizotrons with gel-based media showed that primary and lateral root growth is more extensive in soil (Fig 5B). Interestingly, previous work has suggested that auxin levels in Brachypodium roots is supra-optimal for growth[31]. Our results suggest that gel-based systems may lead to an imbalance in hormone signaling that causes slower growth.

Tomato plants were transformed with *Pro35S:PPyRE8o* and *ProeDR5rev:LUC2* reporters. The plants showed more rapid growth than Arabidopsis or Brachypodium and required fertilizer to prevent obvious signs of stress (reduced growth, anthocyanin accumulation). Root systems were imaged from 14 DAS plants. Roots showed less branching than for Arabidopsis but showed many presumptive lateral root primordia marked by DR5-expression (Fig 5C-D). These results show that the GLO-Roots method is widely applicable to study root systems of plants and will likely be useful for studying root systems of other small to medium sized model and crop plants.

Spectrally distinct luciferases enable characterization of root system interactions, microbial colonization and gene expression patterns.

Although root system architecture is usually studied in isolated plants, this is rarely the case in nature where plants compete for soil resources through root-root interactions. Recent work in this area has suggested that roots from the same cultivar can grow without competition while roots from different cultivars avoid each other[32]. One of the major challenges in such studies is the ability to distinguish two overlapping root systems. We took advantage of our ability to constitutively express two spectrally different luciferases and imaged the overlapping root systems of two Col-0 plants (one expressing *ProUBQ10:LUC2o* and the other *ProACT2:PPy RE8o*) or one Col-0 plant (expressing *ProACT2:PPy RE8o*) and one Sha plant (expressing *ProUBQ10:LUC2o*). Images were captured using unfiltered light and a custom (76.5 mm diameter) band-pass filter (415 nm - 485 nm), which captured

light emitted predominantly by LUC2o. By overlaying the images, we were able to distinguish the two overlapping root systems (Figure 6 Supplement 1). We compared root traits of plants grown together or in isolation but could not observe any significant differences between treatments. This was also observed when Col-0 was grown with the Sha accession. Further studies are warranted, however, as environmental conditions where resources are limited may lead to more competition.

The GLO-Roots system uses non-sterile growth conditions, which allows complex biotic interactions that may affect responses to the environment. Bacteria themselves can be engineered to express luminescent reporters through integration of the LUX operon, which results in luminescence in the blue region of the spectrum and is thus compatible with the plant-expressed luciferase isoforms we have tested. *Pseudomonas fluorescens* CH267[33], a natural Arabidopsis root commensal, was transformed with the bacterial LUX operon and used to inoculate plants. Thirteen days after inoculation we were able to observe bacterial luminescence colocalizing with plant roots. *P. fluorescens* did not show an obvious pattern of colonization at the root system scale level. As a proof-of-principle test of the multi-dimensional capabilities of the GLO-Roots system we visualized both *LUC2o* and *PPyRE8o* reporters in plants and the LUX reporter in bacteria in the same rhizotron (Figure 6).

One of the major advantages of our system is that luciferase reporters have been commonly used to study gene expression and these resources can potentially be utilized to study these regulatory events in soil-grown roots. We transformed *ProACT2:PpyRE8o* into two well studied LUC reporter lines: the auxin activity reporter line *ProDR5:LUC+*[34] (Figure 7A) and the ROS activity reporter *ProZAT12:LUC*[35] (Figure 7B). We implemented in GLO-RIA an algorithm that semi-automatically identifies gene reporter signal and associates this object to the corresponding root structure segment. These two associated variables can be tracked in time lapse experiments. Using the *ProACT2:PpyRE8o* and *ZAT12:LUC* line we tracked root-tip associated changes in growth and reporter expression throughout the whole root system in response to a local application of a 1 M NaCl solution over 24 hours. As shown in Video 2, reporter activity declines rapidly at the site of salt application while

growth and ZAT12 reporter activity become induced further away at later time points and correlates with a burst of growth in this part of the root system (Fig 7E-F).

ADAPTIVE RESPONSES TO SOIL-BASED ENVIRONMENTAL STIMULI

Phosphorus availability promotes shallow root systems To examine the effects of phosphorus availability on RSA we used alumina particles buffered with 100 µM phosphate (P) to supply this macro-nutrient to the root. Alumina particles bind and release inorganic phosphorus similarly to soil particles, thus providing a physiologically relevant nutrient regime[36]. Alumina particles lacking P, which would remove P supplied by the peat-based soil, were used to simulate a P-deficient soil. Root and shoot phenotypes of control and P-deficient plants at 22 (FIg 8A) and 27 (Fig 8B) DAS are shown. Plants grown in low-P soil showed a significant increase in the width-depth ratio of the root system compared to plants grown in P-replete soil, as determined using the automated root system area finder in GLO-RIA (Fig 8). Plants under P deficiency showed an increase in the ratio between root-shoot area (FIgure 8C) and higher investment of resources in the development of the root system at the expense of shoot growth (Figure 8D). Root systems of control and P-deficient plants showed no significant differences in directionality at 22 DAS but at 27 DAS, roots were more horizontally oriented in P-deficient plants (Figure 8E). The observed changes in root architecture are consistent with root system ideotypes that improve phosphorus uptake efficiency.

Light promotes root gravitropism through PHOTOTROPIN signaling To examine the effects of light exposure on the root system, the black shields, which normally protect the soil and roots from light, were removed from the top half of the rhizotron 10 DAS. Using directionality analysis we detected a significant increase in the steepness of roots only in the light exposed region of the rhizotron, while the lower shielded region showed no difference. (Fig 9A-B). Light can penetrate the top layers of soil[37] and it has been proposed to have a role in directing root growth (Figure 9 supplement 1) specially in dry soils[38] trough the blue light receptor *phot1*. Root directionality was not significantly different between light

and dark-treated roots of the *phot1/2* double mutant suggesting that blue light perception is necessary for this response (Fig 9B), which is consistent with previous studies[38,39]. These data highlight the strong effects of light on root system architecture[18], which GLO-Roots rhizotrons are able to mitigate.

Adaptive changes in root system architecture under water deprivation. GLO-Roots provides important advantages over gel-based systems for studying water-deficit (WD) responses. First, shoots are exposed to the atmosphere and vapor pressure deficit (VPD) is maintained at levels that allow for transpiration of water from the shoot. Second, WD can be simulated in more realistic ways than in gel. Soil in rhizotrons is exposed to air at the top and dries basipetally (from the top-down); drying soil increases the volume occupied by air and reduces contact of root with liquid water, all of which are similar to changes in soil expected in the field during WD. Finally, as peat-based soil dries, its optical properties change, allowing moisture content to be approximated from bright-field images. We took advantage of the change in gray-scale pixel intensity to construct a calibration curve (Figure 10 Supplement 1) that quantitatively relates gray-scale pixel intensity to moisture content (Fig 10A); water content can be color coded in images with appropriate look up tables (Fig 10B). Using this approach, water content in a rhizotron can be mapped and visualized in 2D (Fig 10C-D) In the example shown, we can observe that a 22 DAS Bay-0 plant depleted soil-moisture content locally around the the root system (Figure 10E).

We performed several trials to simulate WD in our growth system. Plants were germinated, grown under control conditions then transferred to 29^{o}C and standing water was removed from the container holding the rhizotrons starting at either 9 DAS or 13 DAS. Elevated temperature combined with water deficit is a common stress that modern crops varieties are poorly adapted to, thus highlighting the importance of examining this combined treatment[40,41]. Plants were maintained in this WD regime until 22 DAS when luciferin was added and the plants were imaged. At 13 DAS, lateral roots near the soil surface are already emerged (Video 1, Figure 3A). After 9 days of water deficit treatment, lateral roots showed an increase in gravitropism leading to the development of a root system that was deeper,

more vertically oriented and with more tertiary roots (Fig 11A). Roots of Bay-0 plants showed similar responses though the extent of change was less pronounced since Bay-0 roots are normally more vertically oriented (Fig 11B).Plants transferred at 9 DAS showed less lateral root development in the top layer of soil (Fig 11E). At this time point, lateral roots start to emerge Video 1 and early drought may lead to growth quiescence or senescence. We also grew plants under WD at control temperatures or under WW conditions at high temperature to test the effects water and temperature had on root architecture in isolation. We observed that both conditions were sufficient to induce a change in root directionality indicating that the plant uses similar mechanisms to avoid heat and water-deficit associated stresses (Figure 11 Supplement 1). We next asked which regulatory pathways controlled the observed changes in lateral root directionality during simulated drought. Hydrotropism is a known environmental response that directs root growth towards wet regions of soil. MIZ1 is an essential regulator of hydrotropism; however miz1 mutants had no significant effect on water deficit-induced changes in root directionality, compared to wild type (Fig 11C), indicating that this response was distinct from hydrotropism. Auxin is an important mediator of gravitropism and auxin treatment causes lateral roots to grow more vertically[8]. Consistent with this role for auxin, mutant plants with loss of function in the auxin receptor TIR1, did not show changes in the root system directionality between WW and WD conditions (Fig 11D).

Plants transferred at 9 DAS showed less lateral root development in the top layer of soil.(Fig 11E) At this time point, lateral roots start to emerge (See Video 1) and early drought may lead to growth quiescence or senescence[2]. Careful examination of roots in these regions showed evidence of small lateral root primordia populating parent roots (Figure 11F). After 24 h of re-watering (Figure 11G) these lateral root primordia reinitiated growth (Figure 11H)

Time-lapse imaging of the water deficit response showed that changes in root growth direction occurred ahead of the dry soil front Video 3. Using GLO-RIA we were able correlate water moisture contents with local orientation of the root segments. With this approach we

observed that root segments in dryer areas of rhizotron grew at steeper root angles (Figure 12) than roots in growing in well watered regions, though lateral root angle in wetter regions was also affected. These data suggest that local and systemic signaling is likely involved in redirecting lateral roots deeper during the simulated drought treatments tested here.

Discussion

Organisms have evolved to acclimate to environmental change through adaptive responses. Stressful environmental conditions can elicit tolerance mechanisms that allow the organism to bear the negative effects of sub-optimal conditions while avoidance mechanisms provide alternative routes for acquiring needed resources. Environmental stresses such as phosphate deprivation or water deficit simulated in gel-based systems typically cause a reduction in root growth, suggesting that the plant is preserving resources to ensure survival. Interestingly, simulation of these same stresses using the soil-based GLO-Roots system was able to elicit changes in root growth that are anticipated to provide a mechanism to avoid stress. These data support the utility of GLO-Roots for characterizing environmental responses that are difficult to characterize otherwise.

GLO-Roots enables a multi-dimensional understanding of root biology

Recent studies of root systems has emphasized structural attributes as important contributors of root system function. Indeed, studies examining the role of genetic variants in tolerating abiotic stress have demonstrated the importance of such characteristics. Roots, however, are highly diverse in the biology they perform and a multi-dimensional understanding of root systems, which incorporates differences in signaling, metabolism and microbial association as well as structure, may provide a clearer understanding of the degree to which sub-functionalization of the root system plays a role in important processes such as acclimation and efficient resource acquisition.

We have developed tools in GLO-Roots that allow for tracking multiple aspects of soil physicochemical properties and root biology simultaneously. Using GLO-Roots, we are able

to map in 2D coordinates soil physical properties such soil moisture together with root architecture traits such as directionality, growth rates and gene expression levels. All this information is aggregated in layers for each x, y coordinate. Using GLO-RIA we integrate this multilayer information, leveraging our ability to simultaneously and seamlessly investigate root responses to environmental stimuli such as soil moisture content. Luciferase isoforms that emit light at different wavelengths allow for constitutive and regulated promoters to be studied together. Introduction of luciferase reporters into microbes provides an additional layer of information that provides a readout on the association between organisms and how this might be affected by environmental conditions. The flexibility of the GLO-Roots system may enable additional dimensionality to our understanding of root biology. Other physical properties such as CO_2 or pH mapping in rhizotrons have already been enabled by using planar optodes[42]. It may be possible to engineer LUX-based reporters in microbes that are responsive to extracellular metabolites, creating microbial biosensors, and integration of such tools may enable root-exudation and nutrition to be analyzed in soil. Split-Luciferase reporters have been engineered that allow bi-molecular interactions to be studied. Finally, molecular sensors analogous to FRET sensors, termed BRET-sensors[43], may allow metabolite tracking dynamically through the root system. With additional innovation in the development of luciferase reporters, the GLO-Roots systems will likely expand the repertoire of biological processes that can be studied over an expanded range of developmental time points and environmental conditions.

Limited phosphorus availability promotes foraging in upper-layers of soil

Phosphorus availability is one of the major limitations for plant growth and an important factor influencing root architecture[44]. P is usually more abundant in the top layers of the soil where it is bound to organic matter and clay minerals. Modeling studies have suggested that an increase in lateral root density and shallower root systems promote phosphorus uptake since phosphorus diffusibility is limited in soil and this nutrient tends to accumulate in the upper tiers of the soil column where decomposition of organic matter replenishes the

supply of P[10,45].

Experiments using in vitro grown Arabidopsis seedlings have shown that the primary root will senesce during low-P stress while lateral root growth is enhanced, however the total root system area is often highly reduced. This change in root development would be expected to reduce energy input into the root system, but provide little advantage in absorbing additional phosphorus. Using GLO-Roots, we demonstrate that Arabidopsis does indeed have a robust low-P response that we predict to enhance phosphorus uptake. While root system area is not significantly reduced, root system width-depth ratio is increased, generating a shallower root system. Differences between in vitro and GLO-Roots root systems may be a result of the more physiologically realistic manner in which phosphorus is released to the root when phosphate-buffered alumina particles are used[36].

Enhanced root growth and gravitropism may constitute an avoidance mechanism used during drought

It has been proposed that plants with steep root systems will be better able to tap into deep water resources and thus perform better under water deprivation. For example in rice, the IR64 paddy cultivar shows shallow root systems in upland fields whereas Kinandang Patong, an upland cultivar, is deeper rooting[9]. Plants maintain a number of regulatory pathways that mediate changes in physiology during WD. Enhanced growth of root systems has been well characterized in field-grown plants; however this has not been recapitulated in studies of gel-grown Arabidopsis plants. Thus, it has been unclear whether Arabidopsis simply responds to WD differently. Our results here show that Arabidopsis does indeed maintain a classical WD response that expands the root system and directs growth downward. Interestingly, under our stress regime, we did not observe a significant decrease in the relative water content of shoot tissues (Figure 11 Supplement 2), suggesting that the changes in root architecture were sufficient to provide access to deep water and prevent dehydration. Such changes in root growth are likely regulated through systemic and local signaling that involve auxin signaling but acts independently of known pathways that control moisture-directed

root growth.

Perspectives and Conclusions

Understanding plant biology requires a sophisticated understanding of how environmental stimuli affect the form and function of plants as well as an understanding of how physiological context informs such responses. Environmental conditions are at least as complex as the plants they affect. Plant roots are exposed to a variety of environmental signals that change in time and space at very different scales that are integrated at the whole plant system. It is an important challenge in biology to develop methods of growing and studying plants that present such stimuli in a manner that the plant is likely to encounter in nature. After all, the plants we study have evolved to survive through mechanisms that have been selected, over evolutionary time, in nature. Use of artificial conditions must be carefully considered especially if adaptive mechanisms are the area of focus for the study.

The study presented here shows conclusively that root biology in soil-like media is distinct from in vitro grown plants. These differences are not only due to media composition but likely encompass effects from other abiotic and biotic factors as well. It will be interesting for future studies to determine how other environmental stimuli affect root growth using GLO-Roots and whether these responses differ between accessions of Arabidopsis. Identification of the genetic loci responsible for phenotypic variation in adult root phenotypes may identify the molecular basis for adaptive variation that exists in this species and potentially identify loci that are useful for breeding efforts needed for the next green revolution.

Materials and methods

Growth system

Rhizotrons and growth system fabrication. Rhizotrons are composed of two sheets of 1/8" abrasion resistant polycarbonate plastic (Makrolon AR (R)) cut to size using a water jet (AquaJet LLC, Salem, OR), two acrylic spacers cut using a laser (Stanford Product

Realization Lab), two rubber U-channels cut to strips 30 cm long (McMaster Carr part # 8507K33) and two sheets of black 0.030" thick polypropylene sheets (McMaster Carr part # 1451T21) cut with a straight-edge razor blade. Rhizotron designs were drafted in Adobe Illustrator (Adobe, San José, CA). The blueprints of all the parts are provided in Supplement 1. The top edge of each polycarbonate sheet was painted with black 270 Stiletto nail polish (Revlon, New York, NY).

Boxes and holders. Rhizotrons are held vertical during plant growth in a custom rack system composed of two sheets of 1/4" black acrylic plastic cut with slots for eleven rhizotrons using a laser, four 3/8" PVC rods (McMaster Carr part # 98871a041) secured with PVC nuts (McMaster Carr part # 94806a031) to hold the acrylic sheets horizontal. The rack is placed inside a 12" x 12" x 12" black polyethylene tank (Plastic Mart part # R121212A).

Rhizotron preparation The procedure to construct a rhizotron with soil is as follows: Two pieces of polycarbonate plastic are laid flat on a table with the spacers inserted. Using an electric paint gun, a fine mist of water is applied to the bare polycarbonate sheets. Then, using a 2 mm sieve (US Standard Sieve Series Nº 10) a fine layer of PRO-MIX(r) PGX soil (Premier Tech, Canada) is applied. Excess soil is discarded by gently tapping the plastic against the table in a vertical position. Water is sprayed again onto the soil, then a second layer of Pro-MIX is applied as before. For P deficiency experiments soil supplemented with 1 ml of 100 µM P-Alumina (control) and 0-P-Alumina (P deficient) was used. To prevent the soil from falling out of the bottom opening, a 3 x 6 cm piece of nylon mesh is rolled into a 1 cm wide tube and placed at the bottom side of the rhizotron. The spacers are removed and replaced by clean spacers. The two faces of the rhizotron are carefully joined together and two rubber U-channels slipped on to clamp all pieces together. Assembled rhizotrons are placed into the rack inside the boxes and 500 mL of water is added to the box.

Plant growth *Arabidopsis thaliana* seeds were stratified for 2 d at 4 ºC in Eppendorf tubes with distilled water. Seeds were suspended in 0.1 % agar and 5 to 10 were sown using a transfer pipette in the rhizotron. A transparent acrylic sheet was mounted on top of the box and sealed with tape to ensure high humidity conditions that enable *Arabidopsis*

germination. Three days after sowing, the cover was unsealed to decrease humidity and allow the seedlings to acclimate to a dryer environment. From 3 days after sowing (DAS) to the time the first true leaves emerged, it was critical to ensure that the top part of the rhizotron remained humid for proper germination of the plants. Between three and five DAS the rhizotrons were thinned leaving only the number plants required for that experiment, typically one, except for experiments examining root-root interactions. Unless otherwise stated, all the experiments presented here, treatments were started 10 DAS. Plants were grown under long day conditions (16 h light / 8 h dark) using 20–22 ºC (day/night) and 150 µE m–1 s–1. Two types of growth environments were used for experiments. A walk-in growth chamber with fluorescent lightning and a growth cabinet with white LED lights.

qRT-PCR analysis.

Seeds were surface sterilized as described before[2] and grown in rhizotrons, 100 cm^3 pots, or on two types of 1% agar (Duchefa) media containing either 1x MS nutrients (Caisson) and 1% Sucrose, (termed ms media) or ¼x MS nutrients only (termed ms25 media). Both media were buffered using 0.5 g/L MES and pH was adjusted to 5.7 with KOH. All plants were grown together in a growth cabinet with LED lights under long day conditions (16h day/8h night). Root and shoot tissue was collected separately from individual plants at the end of the day (1 hour before the lights shut off) and at the end of the night (1 hour before lights came on). Three biological replicates were collected for each condition. RNA was extracted using the Plant RNA MiniPrepTM kit (ZYMO Research) according to manufacturer's instructions with on-column DNase treatment (Qiagen). cDNA was made using the iScript Advanced cDNA Synthesis for RT-qPCR kit (Bio-Rad) from 200 ng of total RNA. qRT-PCR was performed using a Fluidigm BioMarkTM 96.96 Dynamic Array IFC with the EvaGreen® (Bio-Rad) fluorescence probe according to the Fluidigm Advanced Development Protocol number 37. For the analysis, all the reactions with no amplification (Ct =999) were either removed (if the other technical duplicate amplified) or set to the maximal Ct for that assay type. The two technical replicates were then averaged and dCt values calculated using

AT3G07480, AT4G37830, At1g13320 and At1g13440 as reference internal controls. PCA plots were generated with Devium Web[46] using log dCt values. Primers used are listed in file Supplement 8.

Biological components

Codon optimization of luciferases. The following luciferases that emit light at different wavelengths were codon optimized for Arabidopsis (Genscript, Piscataway, NJ): LUC2: a yellow improved version (Promega, Madison, WI) of the original *Photinus pyralis* (firefly) LUC.

- Ppy RE8: a red variant[47] of the P. pyralis thermostable variant Ppy RE-TS[48].
- CBG99: a green variant (Promega, Madison, WI) from yellow click beetle (*Pyrophorus plagiophthalamus*) luciferases.
- CBR: a red variant (Promega, Madison, WI) from yellow click beetle.

Non-optimized luciferases. We also used the following non-optimized luciferases:

- nanoLUC: a blue luciferase isolated from a deep sea shrimp[49].
- venusLUC2: a venus-LUC2 fusion reported to show higher luminescence output than LUC2[24].
- A transposon containing the bacterial luciferase-containing LUX operon was integrated into the *Pseudomonas fluorescens* CH267[33] genome by conjugation with *E. coli SM10 pir* containing pUT-EM7-LUX[50] and used to track root microbe colonization. For inoculation 9 DAS plants were inoculated with 2 mL of an overnight bacterial culture resuspended in 10 mM MgSO~4 and diluted to 0.01 OD.

Generation of single-reporter transgenic plants. We generated transcriptional fusions of all luciferases to constitutive promoters to examine the activity level and emission spectrum of each isoform. The *attL1-att*L2* entry clones containing plant-codon optimized coding sequence of *LUC2*, *PpyRe8*, *CBG99* and *CBR* were synthesized by Genscript. A DNA fragment including the *UBQ10* promoter region and first intron was amplified from Col–0 genomic DNA with primers incorporating the attB1, attB4 combination sites at the 5' and 3' respectively. The PCR product was then introduced into pDONR™ P4-P1R (Invitrogen) through a classic Gateway BP-reaction. The resulting plasmid, the *attL1-attL2* entry clones with luciferase sequences, an empty *att*R2-attL3* entry clone and the destination vector dpGreenmCherry[2] were used to construct *ProUBQ10*:LUC2o, *ProUBQ10:PpyRE8o*, *ProUBQ10:CBG99o* and *ProUBQ10:CBRo* through Gateway LR reactions. The destination vector *dpGreenmCherry* contains a plasma membrane-localized mCherry coding sequence driven by the 35S promoter and is used as a selectable marker of transformation at the mature seed stage[2]. We used Golden Gate cloning and the destination vectors that we had generated before[25] for the following fusions: *ProUBQ10:nanoLUC2*, *ProUBQ10*:venusLUC, ProACT2*:PpyRE8o*. Briefly, the different components of each construct were PCR amplified with complementary BsaI or SapI cutting sites, mixed with the destination vector in a single tube, digested with either BsaI or SapI, ligated with T4 DNA ligase, then transformed into E. coli Top10 cells and plated on LB antibiotic plates containing X-gal as previously described[25]. Junction sites were confirmed by sequencing. We used pSE7 (Addgene ID #: pGoldenGate-SE7: 47676) as the destination vector of the *ProUBQ10:nanoLUC2*, *ProUBQ10:venusLUC* constructs and pMYC2 (Addgene ID #: pGoldenGate-MCY2: 47679) as the destination vector for *ProACT2:PpyRE8o*. Maps of all the vectors can be found in Supplement 8. *ProUBQ10:LUC2o* was transformed into Col-0, Bay and Sha accessions, the *tir1-1*[51] mutant and the *miz1*[52] T-DNA insertion line (SALK_126928).

Brachypodium distachyon The Arabidopsis plant-codon optimized Luciferase gene, *LUC2o*, was inserted into the monocot vector pANIC10 *via* Gateway cloning[30]. *Brachypodium distachyon* plants were transformed using the method of Vogel and Hill[53].

Tomato The transcriptional fusion *ProeDR5:LUC2* was generated by cloning the *ProeDR5:LUC2* DNA fragment into the pBIB expression vector via restriction sites SalI and Acc65I. The eDR5 promoter is an enhanced version of DR5 containing 13 repeats of the 11-nucleotide core DR5 element[54] and the pBIB expression vector contains an NPTII resistance gene under the control of the NOS promoter for use as a selectable marker during transformation. This construct was transformed into the XYZ cultivar of tomato.

Generation of dual-reporter plants.

To generate dual-reporter plants expressing luciferase isoforms that emit light with divergent emission spectra we used *ProACT2:PpyRE8o* as the root structural marker and ZAT12:LUC[35] and DR5:LUC+[34] lines that were transformed with the *ProACT2:PpyRE8o* construct. All constructs were transformed using a modified floral dip method as described in[2].

Tomato

The *Pro35S:PpyRE8o* transcriptional fusion was generated by putting the plant-codon optimized coding sequence described above into the pMDC32 expression vector through a Gateway LR reaction. The pMDC32 vector contains a hygromycin resistance gene under the control of the 35S promoter for use as a selectable marker during transformation. This construct was transformed into the transgenic *ProeDR5:LUC2* tomato line. All tomato transformations were performed by the Ralph M. Parsons Foundation Plant Transformation Facility (University of California, Davis).

In vivo emission spectra of plants constitutively expressing luciferase isoforms.

To generate *in vivo* emission spectra of all constitutively expressed luciferases, seeds were sterilized and sown on MS plates as described before[2]. After 8 days, seedlings were treated with a 100 µM luciferin solution, incubated at room temperature for 3 hours and imaged using an IVIS Spectrum imaging system (Perkin Elmer, bla, bla) using 20 nm band-pass emission filters at the following wavelengths (in nm: 490-510, 510-530, 530-550, 550-570,

570-590, 590-610, 610-630, 630-650, 650-670, 670-690, 690-710). Raw images were analyzed using Fiji and in vivo emission spectra were constructed. The full emission spectra of LUX and nanoLUC could not be constructed since the maximum of these two luciferases is below the lower band pass filter that were available.

Imaging system

We designed a custom imaging system (GLO1, Growth and Luminescence Observatory 1) optimized for imaging dual-reporter luciferase expression in our custom rhizotrons. The design was a joint effort with Bioimaging Solutions (San Diego, CA) who also built the system and wrote the acquisition software that drives all the mechanical parts of the system. The system is composed by two 2048 x 2048 PIXIS-XB cameras (Princeton Instruments, Trenton, NJ) mounted on top of each other to capture two fields of view encompassing approximately two 15 x 15 cm areas corresponding to the top or bottom of the rhizotron. The cameras are fitted with a Carl-Zeiss macro lens. A filter wheel with space for four, 76.2 mm filters is positioned in front of the cameras and controlled by a stepper motor allowing for automated changing of the filter wheel position. We used two -542/50 and 450/70- custom cut Brightline(R) band-pass filters (Semrock, Rochester, NY). In single color imaging mode, the filter wheel is operated without filters. Positioned in front of the filter wheel is a removable rhizotron holder mounted on a stepper motor. This stepper motor is also controlled by the GLO-1 software allowing automatic acquisition of images from both sides of the rhizotron sequentially. The whole imaging system is enclosed in a light-tight black box with a door that allows loading and un-loading of rhizotrons.

Plant Imaging

Around 50 mL of 300 µM D-luciferin (Biosynth, Itasca, IL) was added to soil at the top of the rhizotron. In general 5 min exposures were taken per rhizotron, per side, per channel. For daily imaging experiments, plants were imaged at dawn (+/- 1 hr) to reduce possible effects on diurnal rhythms of keeping plants in the dark during imaging. Shoot images were

taken using a Nikon D3100 camera.

Image Preparation

Four individual images are collected: top front, bottom front, top back and bottom back and a composite image is generated as follows: 1)To correct for differences in background values between the two cameras the mean background value of each image is subtracted from 200; 2) images are rotated and translated to control for small misalignments between the two cameras; 3) the top and bottom images of each side are merged; 4) the back image is flipped horizontally; 5) the front and back images are combined using the maximum values. When dual color images are acquired this operation is repeated for each channel. The final images produced are 16-bit depth and 4096 x 2048 pixels. The scale of the images is 138.6 pixels per cm. Considering that an Arabidopsis roots is 100 µm this results in 1.39 pixels across an Arabidopsis root.

GLO-RIA imageJ plug-in

The GLO-RIA plugin is divided in two parts:

The first part (RootSystem) performs four different types of analysis: i) local analysis detects all root particles in the image and computes their position, length and direction; ii) the global analysis performs a root system level analysis and computes the total visible surface, convex hull, width and depth; iii) the shape analysis uses Elliptic Fourier Descriptors to perform a shape analysis on the root system convex hull iv) the directionality analysis computes the mean direction of root particles in a root system (either on the full image or by user-defined sections of the image). These four analysis are fully automated by default, but can be manually adjusted if needed.

The second part of GLO-RIA (RootReporter) was specifically designed for the analysis of dual reporter images (gene reporter and a root structural reporter). Shortly, the plugin works as follow: i) detection of the gene reporters and the structure reporters in their

respective images; ii) if needed, a manual correction can be performed to correct the automated detection; iii) gene reporters are linked with the structure reporters, based on their proximity; iv) gene reporter intensity (either absolute or normalized using the structural reporter) is computed; v) all data are exported and saved to an RSML datafile[55]. Gene and structure reporters can be followed across different time and space points. The code source for the plugin, manual and sample images can be found in the github repository of the project.

Statistical analysis was performed in R[56]. The tidyr[57], dplyr[57], gridExtra[58] and ggplot2[59] packages were used for data preparation, analysis and plotting. Final figure preparation was done in Inkscape.

Data availability

All the scripts and orginal data used to analyze and produce the images can be accessed in the Github repository of the project: github.com/rr-lab/glo_roots. Raw files of all the images used in the paper is availabe in Dryad.

Acknowledgements

Work in the lab of JRD was funded by the Carnegie Institution for Science Endowment and grants from the National Science Foundation (MCB-115795) and Department of Energy, Biological and Environmental Research program (DE-SC0008769). RRA was supported by a Carnegie Postdoc Fellowship and currently by Conacyt Ciencia Básica Joven Investigador grant number (CB-2014-01-238101). GL was supported by the Belgian Fonds de la Recherche Scientifique. JM was funded by the National Science Foundation (IOS-0820854). CH is funded by MGH Toteston & Fund for Medical Discovery Fellowship grant 2014A051303 and NIH R37 grant GM48707 and NSF grant MCB-0519898 awarded to Frederick Ausubel, and previously by the Gordon and Betty Moore Foundation through Grant GBMF 2550.01 from the Life Sciences Research Foundation. JV was funded by the Office

of Biological and Environmental Research, Office of Science, US Department of Energy, interagency agreements DE-SC0001526 and DE-AI02-07ER64452. We thank Robert Mittler and Philip Benfey for providing seeds of ZAT12:LUC and DR5:LUC+ respectively. We also thank Neil Robbins for critical review of the manuscript an suggestions during the development of the project.

Competing interests

We do not have any competing interests that we are aware of.

Tables

Table 1: Luciferases used in this study.

Luciferase	Origin	maximum wavelength	Substrate
Ppy RE8	firefly	618	D-luciferin
CBGRed	click beetle	615	D-luciferin
venus-LUC2	FP + firefly	580	D-luciferin
LUC(+)	firefly	578	D-luciferin
CBG99	click beetle	537	D-luciferin
lux operon	A. fischeri	490	biosynthesis pathway encoded within operon
nanoLUC	Deep sea shrimp	470	furimazine

References

1.Dinneny, J. R. *et al.* Cell identity mediates the response of *Arabidopsis* roots to abiotic stress. *Science* **320,** 942–945 (2008).

2.Duan, L. *et al.* Endodermal ABA Signaling Promotes Lateral Root Quiescence during Salt Stress in Arabidopsis Seedlings. *Plant Cell* **25,** 324–341 (2013).

3.Lynch, J. P. & Wojciechowski, T. Opportunities and challenges in the subsoil: pathways to deeper rooted crops. *J. Exp. Bot.* (2015).

4.Brady, N. C. & Weil, R. R. *Elements of the nature and properties of soils.* (Prentice Hall, 2009).

5.Bao, Y. *et al.* Plant roots use a patterning mechanism to position lateral root branches toward available water. *Proc Natl Acad Sci* **111,** 9319–9324 (2014).

6.Tabata, R. *et al.* Perception of root-derived peptides by shoot LRR-RKs mediates systemic N-demand signaling. *Science* **346,** 343–346 (2014).

7.Marschner, P. *Marschner's Mineral Nutrition of Higher Plants.* (Academic Press, 2012).

8.Rosquete, M. R. *et al.* An Auxin Transport Mechanism Restricts Positive Orthogravitropism in Lateral Roots. *Current Biology* **23,** 817–822 (2013).

9.Uga, Y. *et al.* Control of root system architecture by DEEPER ROOTING 1 increases rice yield under drought conditions. *Nat. Genet.* – (2013).

10.Postma, J. A. & Lynch, J. P. The optimal lateral root branching density for maize depends on nitrogen and phosphorus availability. *Plant Physiol.* 1–34 (2014).

11.Kellermeier, F. *et al.* Analysis of the Root System Architecture of Arabidopsis Provides a Quantitative Readout of Crosstalk between Nutritional Signals. *The Plant Cell* **26,** 1480–1496 (2014).

12.Giehl, R. F., Lima, J. E. & Wirén, N. von. Localized iron supply triggers lateral root elongation in arabidopsis by altering the *AUX1*-mediated auxin distribution. *Plant Cell* (2012).

961 13.Galvan-Ampudia, C. S. *et al.* Halotropism Is a Response of Plant Roots to Avoid a Saline
962 Environment. *Current Biology* 1–7 (2013).

963 14.Geng, Y. *et al.* A spatio-temporal understanding of growth regulation during the salt
964 stress response in Arabidopsis. *Plant Cell* **25,** 2132–2154 (2013).

965 15.Slovak, R. *et al.* A Scalable Open-Source Pipeline for Large-Scale Root Phenotyping of
966 Arabidopsis. *Plant Cell* **26,** tpc.114.124032–2403 (2014).

967 16.Moore, C. R. *et al.* High-throughput computer vision introduces the time axis to a
968 quantitative trait map of a plant growth response. *Genetics* **195,** 1077–1086 (2013).

969 17.Topp, C. N. & Iyer-Pascuzzi, A. S. 3D phenotyping and quantitative trait locus mapping
970 identify core regions of the rice genome controlling root architecture. in *Proceedings of the*
971 *…* (2013).

972 18.Yokawa, K., Kagenishi, T. & Baluška, F. Root photomorphogenesis in laboratory-
973 maintained Arabidopsis seedlings. *Trends Plant Sci.* **18,** 117–119 (2013).

974 19.Bucksch, A. *et al.* Image-based high-throughput field phenotyping of crop roots. *Plant*
975 *Physiol.* **166,** 470–486 (2014).

976 20.Trachsel, S., Kaeppler, S. M., Brown, K. M. & Lynch, J. P. Shovelomics: high throughput
977 phenotyping of maize (Zea mays L.) root architecture in the field. *Plant Soil* **341,** 75–87
978 (2011).

979 21.Devienne-Barret, F., Richard-Molard, C., Chelle, M., Maury, O. & Ney, B. Ara-
980 Rhizotron: an effective culture system to study simultaneously root and shoot development
981 of *Arabidopsis*. *Plant Soil* **280,** 253–266 (2006).

982 22.Tracy, S. R. *et al.* Quantifying the impact of soil compaction on root system architecture
983 in tomato (Solanum lycopersicum) by X-ray micro-computed tomography. *Annals of Botany*
984 **110,** 511–519 (2012).

985 23.Grunewald, W. *et al.* Transcription factor WRKY23 assists auxin distribution patterns
986 during Arabidopsis root development through local control on flavonol biosynthesis. *Proc*

987 *Natl Acad Sci* **109,** 1554–1559 (2012).

988 24.Hara-Miyauchi, C. *et al.* Bioluminescent system for dynamic imaging of cell and animal
989 behavior. *Biochem. Biophys. Res. Commun.* **419,** 188–193 (2012).

990 25.Emami, S., Yee, M.-C. & Dinneny, J. R. A robust family of Golden Gate Agrobacterium
991 vectors for plant synthetic biology. *Front. Plant Sc.* **4,** 339 (2013).

992 26.Lindeboom, J. J. *et al.* A Mechanism for Reorientation of Cortical Microtubule Arrays
993 Driven by Microtubule Severing. *Science* **342,** 1245533–1245533 (2013).

994 27.Meijon, M., Satbhai, S. B., Tsuchimatsu, T. & Busch, W. Genome-wide association
995 study using cellular traits identifies a new regulator of root development in. *Nat. Genet.*
996 1–7 (2013).

997 28.Pacheco-Villalobos, D. & Hardtke, C. S. Natural genetic variation of root system archi-
998 tecture from Arabidopsis to Brachypodium: towards adaptive value. *Philosophical Trans-*
999 *actions of the Royal Society of London B: Biological Sciences* **367,** 1552–1558 (2012).

1000 29.Watt, M., Schneebeli, K., Dong, P. & Wilson, I. W. The shoot and root growth of
1001 Brachypodium and its potential as a model for wheat and other cereal crops. *Functional*
1002 *Plant Biol.* **36,** 960–969 (2009).

1003 30.Mann, D. G. J. *et al.* Gateway-compatible vectors for high-throughput gene functional
1004 analysis in switchgrass (Panicum virgatum L.) and other monocot species. *Plant Biotechnol.*
1005 *J.* **10,** 226–236 (2012).

1006 31.Pacheco-Villalobos, D., Sankar, M., Ljung, K. & Hardtke, C. S. Disturbed Local
1007 Auxin Homeostasis Enhances Cellular Anisotropy and Reveals Alternative Wiring of
1008 Auxin-ethylene Crosstalk in Brachypodium distachyon Seminal Roots. *PLoS Genet* **9,**
1009 e1003564 (2013).

1010 32.Fang, S. *et al.* Genotypic recognition and spatial responses by rice roots. *Proc Natl Acad*
1011 *Sci* (2013).

1012 33.Haney, S., C. H. & Ausubel, F. M. Associations with rhizosphere bacteria can confer an

adaptive advantage to plants. *Nature Plants* **In Press,** 0–0 (2015).

34.Moreno-Risueno, M. A. *et al.* Oscillating gene expression determines competence for periodic *Arabidopsis* root branching. *Science* **329,** 1306–1311 (2010).

35.Miller, G. *et al.* The plant NADPH oxidase RBOHD mediates rapid systemic signaling in response to diverse stimuli. *Science Signaling* **2,** ra45 (2009).

36.Lynch, J., Brown, K. & Snyder, R. Controlled release fertilizer comprising modified alumina having phosphorous bound to alumina surface. (2001). at <http://www.google.com.ar/patents/US6287357>

37.Mandoli, D. F., FORD, G. A., WALDRON, L. J., NEMSON, J. A. & Briggs, W. R. Some spectral properties of several soil types: implications for photomorphogenesis*. *Plant Cell Environ.* **13,** 287–294 (1990).

38.Galen, C., Rabenold, J. J. & Liscum, E. Functional ecology of a blue light photoreceptor: effects of phototropin-1 on root growth enhance drought tolerance in Arabidopsis thaliana. *New Phytol.* **173,** 91–99 (2007).

39.Moni, A., Lee, A. Y., Briggs, W. R. & Han, I. S. The blue light receptor Phototropin 1 suppresses lateral root growth by controlling cell elongation. *Plant Biology* n/a–n/a (2014).

40.Lobell, D. B. *et al.* Greater Sensitivity to Drought Accompanies Maize Yield Increase in the U.S. Midwest. *Science* **344,** 516–519 (2014).

41.Ort, D. R. & Long, S. P. Limits on Yields in the Corn Belt. *Science* **344,** 484–485 (2014).

42.Blossfeld, S., Schreiber, C. M., Liebsch, G., Kuhn, A. J. & Hinsinger, P. Quantitative imaging of rhizosphere pH and CO2 dynamics with planar optodes. *Annals of Botany* (2013).

43.Shaw, S. L. & Ehrhardt, D. W. Smaller, Faster, Brighter: Advances in Optical Imaging of Living Plant Cells. *http://dx.doi.org/10.1146/annurev-arplant-042110-103843* **64,** 351–375 (2013).

44.López-Arredondo, D. L., Leyva-González, M. A., González-Morales, S. I., López-Bucio, J.

& Herrera-Estrella, L. Phosphate Nutrition: Improving Low-Phosphate Tolerance in Crops. *Annu. Rev. Plant Biol.* **65,** 95–123 (2014).

45.Lynch, J. P. Root phenes for enhanced soil exploration and phosphorus acquisition: tools for future crops. *Plant Physiol.* **156,** 1041–1049 (2011).

46.Grapov, D. DeviumWeb: Dynamic Multivariate Data Analysis and Visualization Platform.

47.Branchini, B. R. *et al.* Red-emitting luciferases for bioluminescence reporter and imaging applications. *Analytical Biochemistry* **396,** 290–297 (2010).

48.Branchini, B. R. *et al.* Thermostable red and green light-producing firefly luciferase mutants for bioluminescent reporter applications. *Analytical Biochemistry* **361,** 253–262 (2007).

49.Hall, M. P. *et al.* Engineered Luciferase Reporter from a Deep Sea Shrimp Utilizing a Novel Imidazopyrazinone Substrate. *ACS Chem. Biol.* (2012).

50.Lane, M. C., Alteri, C. J., Smith, S. N. & Mobley, H. L. T. Expression of flagella is coincident with uropathogenic Escherichia coli ascension to the upper urinary tract. *Proc. Natl. Acad. Sci. U.S.A.* **104,** 16669–16674 (2007).

51.Ruegger, M. *et al.* The TIR1 protein of Arabidopsis functions in auxin response and is related to human SKP2 and yeast grr1p. *Genes Dev* **12,** 198–207 (1998).

52.Moriwaki, T. *et al.* Hormonal Regulation of Lateral Root Development in Arabidopsis Modulated by MIZ1 and Requirement of GNOM Activity for MIZ1 Function. *Plant Physiol.* **157,** 1209–1220 (2011).

53.Vogel, J. & Hill, T. High-efficiency Agrobacterium-mediated transformation of Brachypodium distachyon inbred line Bd21-3. *Plant Cell Rep* **27,** 471–478 (2008).

54.Covington, M. F. & Harmer, S. L. The Circadian Clock Regulates Auxin Signaling and Responses in Arabidopsis. *Plos Biol* **5,** e222 (2007).

1064 55.Lobet, G. *et al.* Root System Markup Language: toward a unified root architecture
1065 description language. *Plant Physiol.* pp.114.253625 (2015).

1066 56.R Core Team. *R: A language and environment for statistical computing.* (R Foundation
1067 for Statistical Computing, 2014). at <http://www.R-project.org/>

1068 57.Wickham, H. *Tidyr: Easily tidy data with spread() and gather() functions.* (2014). at
1069 <http://CRAN.R-project.org/package=tidyr>

1070 58.Auguie, B. *GridExtra: Functions in grid graphics.* (2012). at <http://CRAN.R-project.
1071 org/package=gridExtra>

1072 59.Wickham, H. *Ggplot2: Elegant graphics for data analysis.* (Springer New York, 2009).
1073 at <http://had.co.nz/ggplot2/book>

Figures

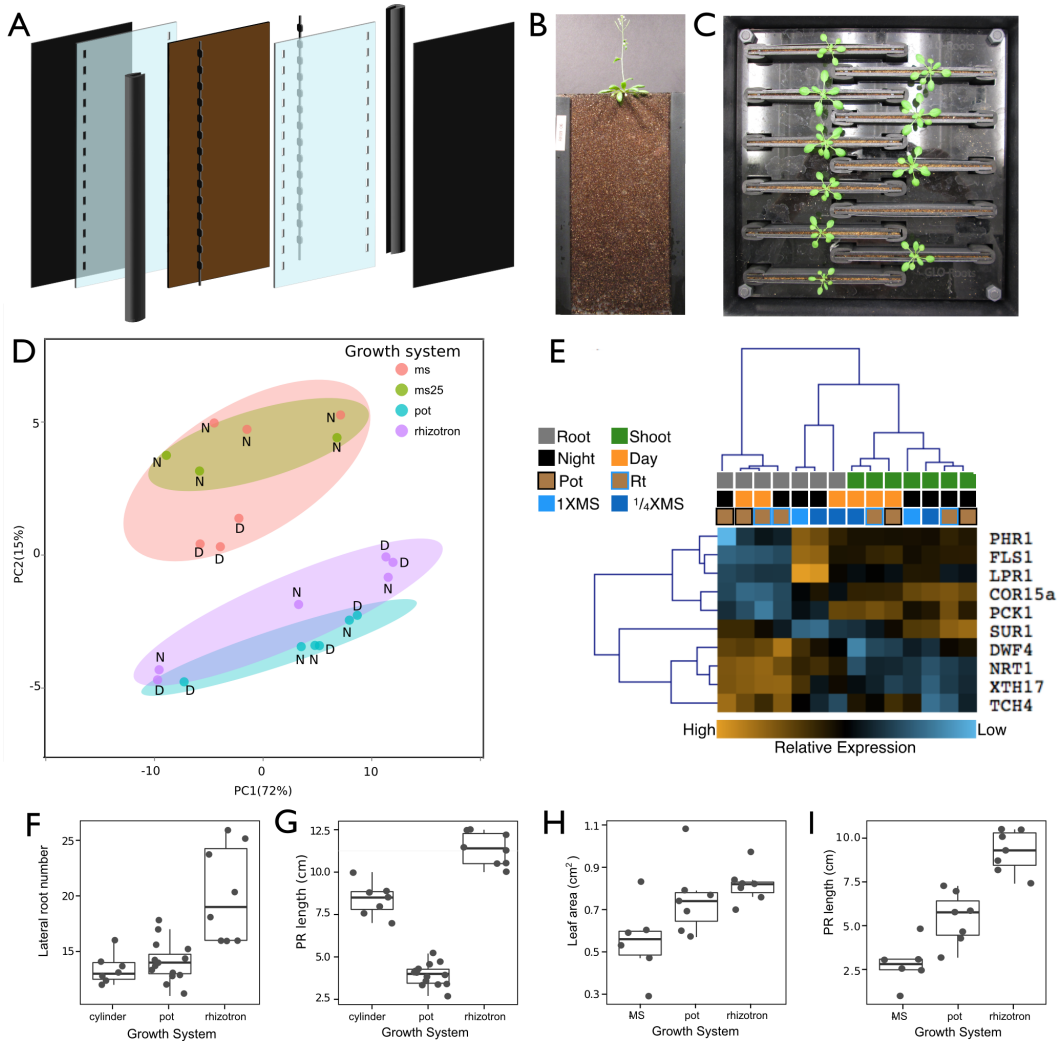

Figure 1. A) 3D representation of the different components of the rhizotron: plastic covers, polycarbonate sheets, spacers and rubber U-channels. Blueprints are provided in Supplementary material 1. In brown, soil layer. B) Thirty five days old plant in rhizotron with black covers removed. C) Top view of holding box with eleven rhizotrons. D) Principal Components Analysis (PCA) score plot of a set of 77 genes analyzed by qPCR from root samples of plants grown in MS plates, pots, and rhizotrons. After 15 DAS three plants were collected at the end of the day (D) and three were collected at the end of the night (N). (ms = plant grown in full ms, ms25 = plants grown in 25% of full ms) E) Heat map of

genes that were significantly different between rhizotrons and media in either day or night or both. We used p-value < 0.00065 threshold based on Bonferoni adjustment for multiple testing. F) Lateral root number and G) primary root length of 18 DAS plants grown in 30 cm tall cylinders, pots and rhizotrons, all with a volume of 100 cm^3 (n = 6-12 plants). H) Leaf area and I) primary root length of plants of the same age (15 DAS) as the ones used for the qPCR experiment (n= 6-7). ANOVA analysis with $p < 0.01$ was used to test significant differences between the different parameters.

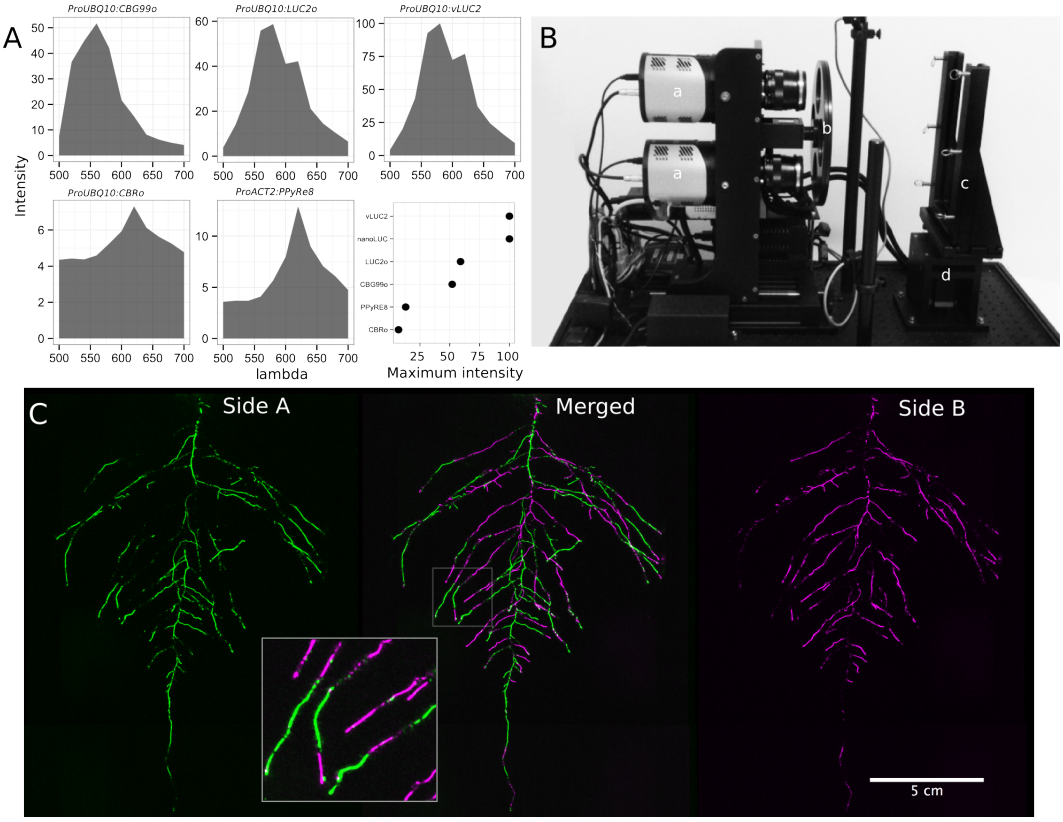

Figure 2: A)In vivo emission spectra of different luciferases used in this study. Transgenic homozygous lines expressing the indicated transgenes were grown on agar media for 8 days. Luciferin (300 µM) was sprayed on the seedlings and plates were kept in the dark and then imaged for 2 s at wavelengths ranging from 500 to 700 nm. Five intensity values were taken from different parts of the roots of different seedlings and averaged. Relative maximum intensity values are indicated in the lower right graph. B) GLO 1 imaging system. The

system is composed by two back illuminated CCD cameras (a) cooled down to -55 ºC. A filter wheel (b) allows for spectral separation of the different luciferases. On the right, a rhizotron holder (c) is used to position the rhizotrons in front of the cameras. A stepper motor (d) rotates the rhizotron 180º to image both sides. C) A 21 DAS plant expressing *ProUBQ10:LUC2o* was imaged on each of two sides of the rhizotron; luminescence signal is colorized in green or magenta to indicate side. In the middle of the panel, a combined image of the two sides is shown. The inset shows a magnified part of the root system. FW: fresh weight, PR: Primary root.

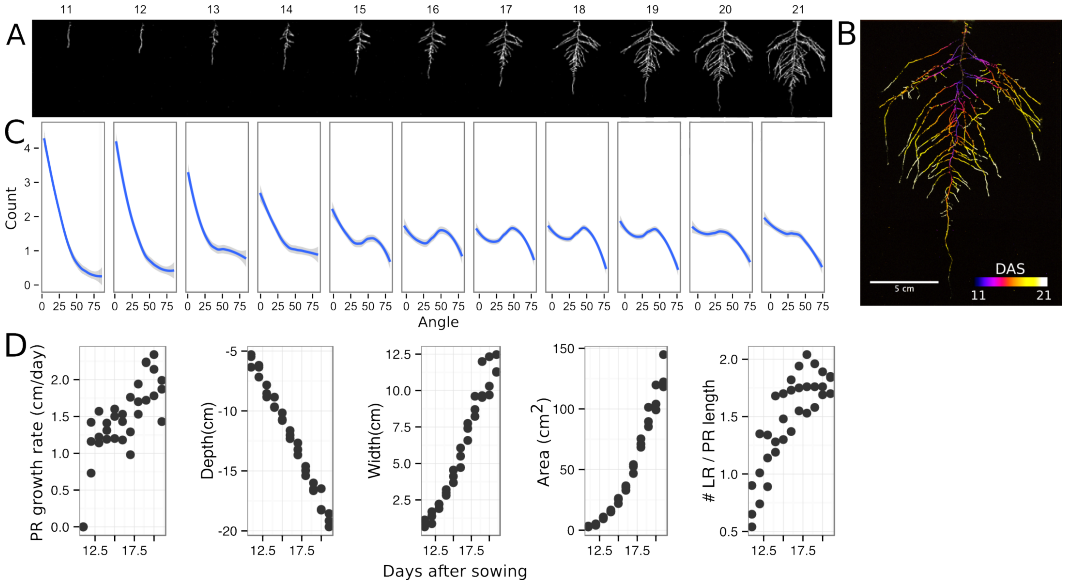

Figure 3. A) Typical daily time-lapse image series from 11 to 21 DAS of a *ProUBQ10:LUC2o* Col-0 plant. B) Color coded projection of root growth using the images in panel A. C) Directionality of the root system of plants in panel A calculated using the directionality plugin implemented in GLO-RIA. D) Primary root growth rate, depth, width, root system area are automatically calculated from the convex hull, which is semi-automatically determined with GLO-RIA. Lateral root number and number of lateral roots divided by the primary root length were quantified manually.A Local Polynomial Regression Fitting with 95% confidence interval (grey) was used to represent the directionality distribution curve. (0º is the direction of the gravity vector).

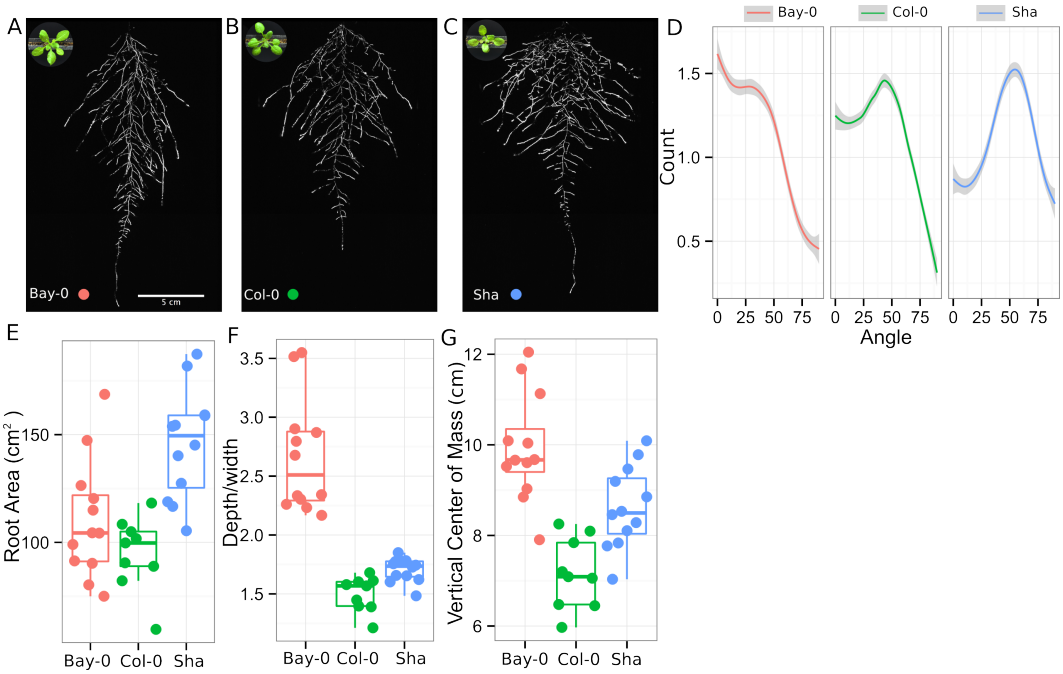

Figure 4: Representative root and shoot images of A) Bay-0, B) Col-0 and C) Sha accessions 22 DAS transformed with *ProUBQ10:LUC2o*. D) Directionality of the root systems, E) root area, F) depth/width ratio G) vertical center of mass of Bay-0, Col-0 and Sha accessions. ANOVA analysis with $p < 0.01$ was used to test significant differences between the different parameters (n = 9-12 plants). A Local Polynomial Regression Fitting with 95% confidence interval (grey) was used to represent the directionality distribution curve. (0^o is the direction of the gravity vector).

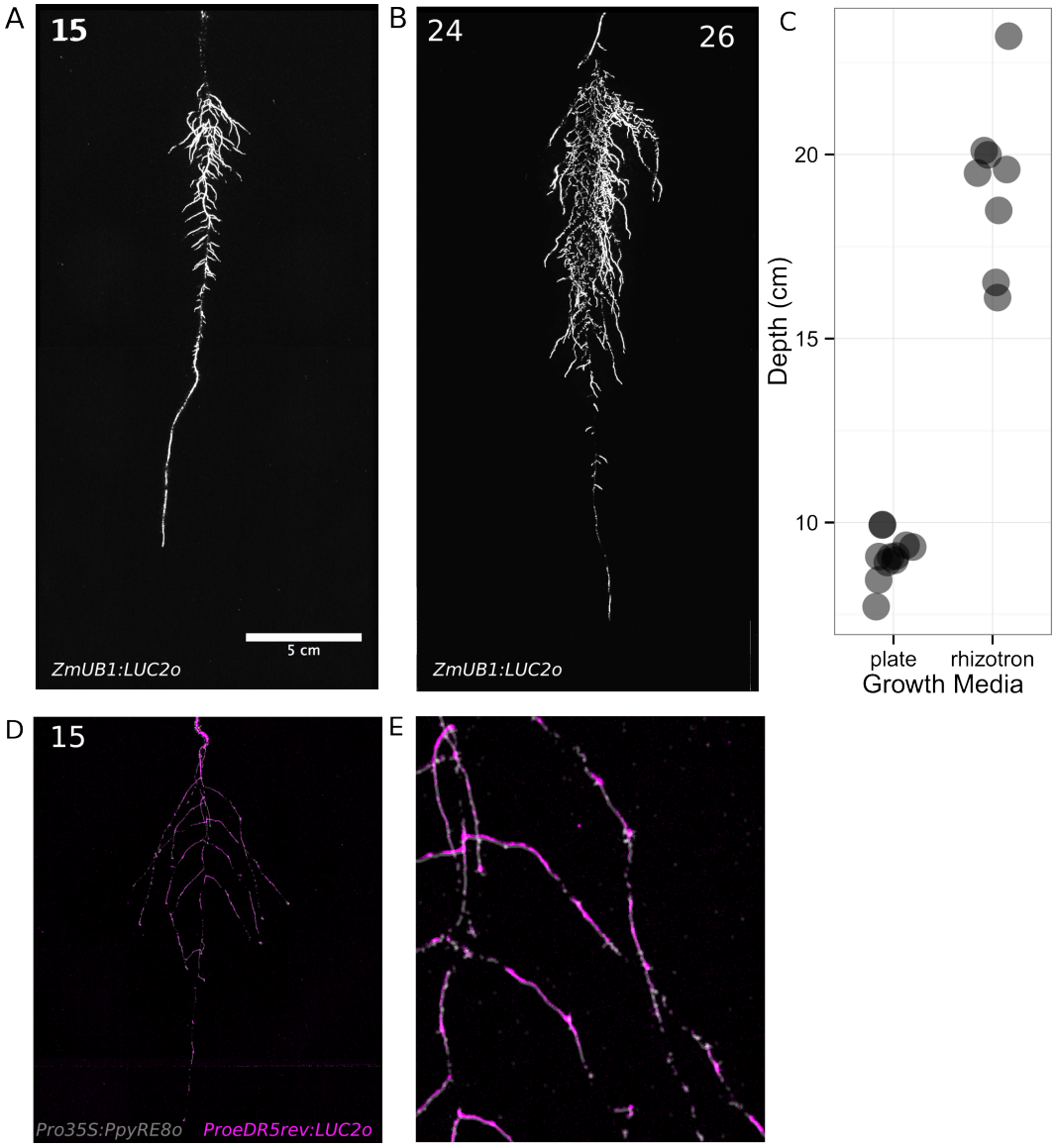

Figure 5: Roots of *Brachypodium distachyon* transformed with *ProZmUB1:LUC2o* and imaged at 15 (A) and 24 (B) DAS grown in control conditions. B) Depth of the primary root of Brachypodium plants grown in rhizotrons or on gel-based media (n=8-11). C) 14 DAS tomato plant transformed with *ProeDR5rev:LUC2o* (magenta) and *Pro35S:PPyRE8o* (grey) D) Zoomed inset of root in panel D showing increased expression of_ ProeDR5rev:LUC2o_ reporter in early-stage lateral roots.

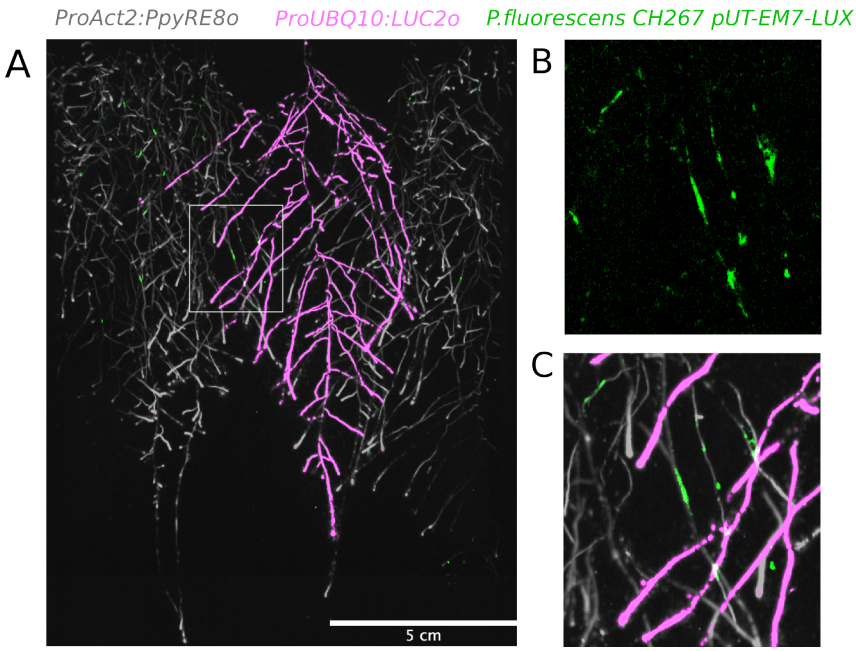

Figure 6: A) Triple color picture showing a 22 DAS *ProUBQ10:LUC2o* plant (magenta) grown in the same rhizotron with *ProACT2:PpyRE8o* plants (grey). Plants were inoculated with *Pseudomonas fluorescens CH267* (green) Magnified portion of root systems colonized by *Pseudomonas fluorescens* showing *P. fluorescences* (B) only or all three reporters together (C).

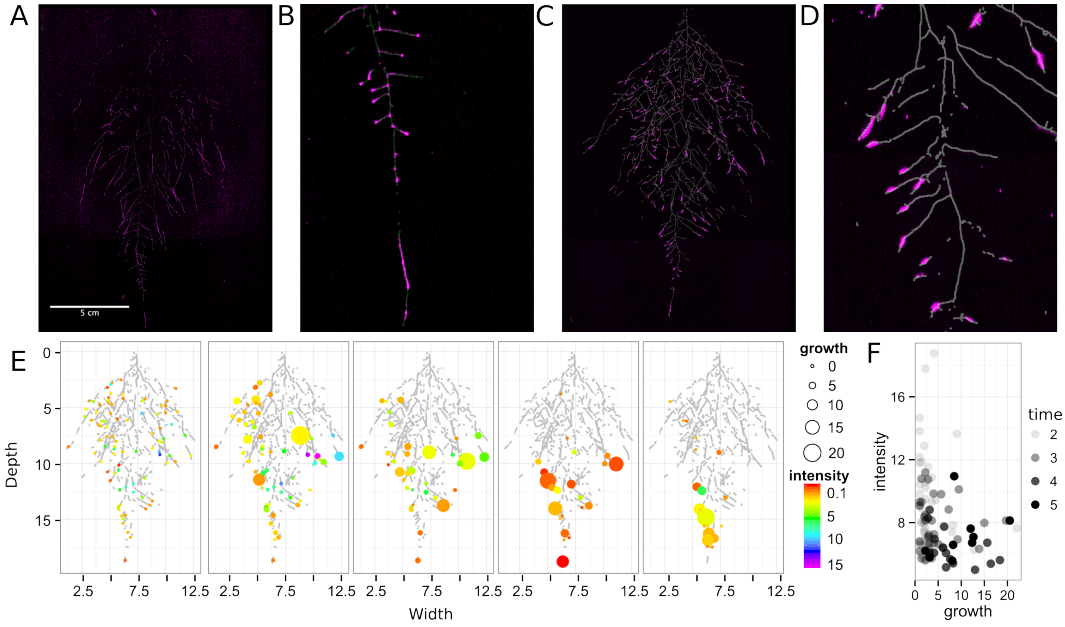

836

837 **Figure 7**: Images of whole root systems (A, C) or magnified portion of roots (B, D) at 22
838 DAS expressing *ProDR5rev:LUC+* (magenta, A, B) or *ProZAT12:LUC* signal (magenta, C,
839 D)with skeletonized representation of root generated using the *ProACT2:PpyRE8o* reporter
840 expression (in grey)) E) Time series showing root growth and *ProZAT12:LUC* expression
841 after salt addition to the right side of the root system. F) Correlation of root growth and
842 *ProZAT12:LUC* expression intensity.

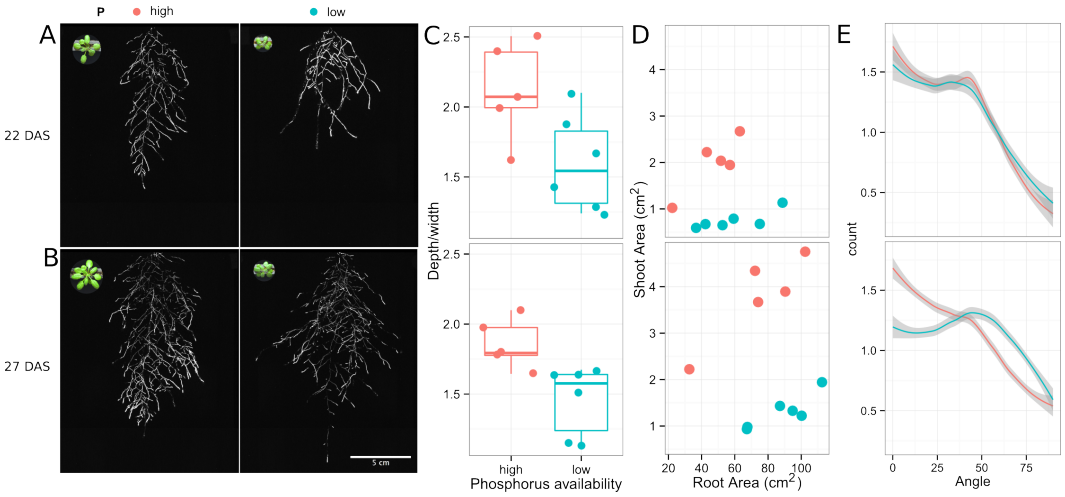

843

844 **Figure 8**. Shoot and root systems of *ProUBQ10:LUC2o* Col-0 plants growing in soil sup-

plemented with 1ml of 100 µM P-Alumina (left) and 0-P-Alumina (right) 22 (A) or 27 (B) DAS. C) Root depth/width ratio of 22 (top) and 27 (bottom) DAS plants. D) Scatter-plot showing relationship between root and shoot system area at 22 (top) and 27 (bottom) DAS. E) Root directionality distribution in plants 22 (top) and 27 (bottom) DAS. Anova analysis at $p < 0.01$ was used to compare depth/width ratios in P treatments. Kolmogorov-Smirnov test at $p < 0.001$ was used to compare directionality distributions between the different treatments. A Local Polynomial Regression Fitting with 95% confidence interval (grey) was used to represent the directionality distribution curve.(0^o is the direction of the gravity vector).

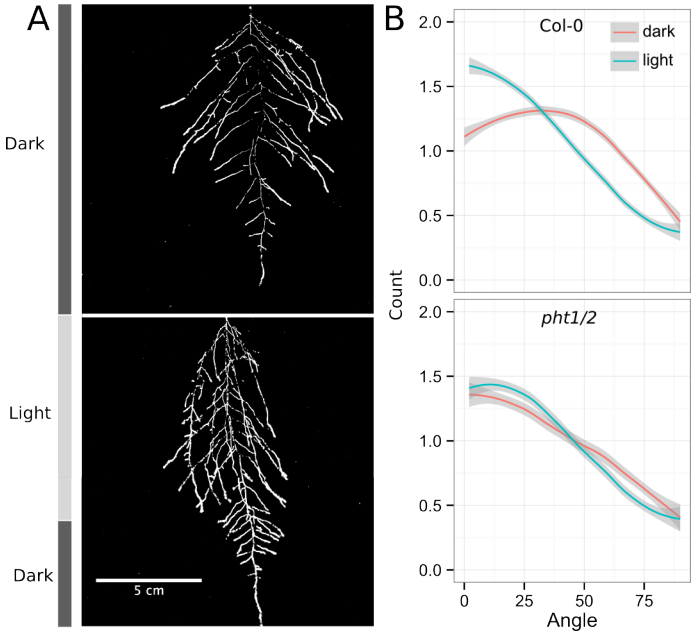

Figure 9. A) Col-0 root systems shielded (top) or light exposed (bottom). After 9 DAS the top third of the rhizotron was exposed to light (indicated on the side with a light grey bar) and plants were imaged at 20 DAS. B) Directionality analysis of root systems shielded (red) or exposed (green) to light for Col-0 (top panel) or phot1/2 double mutant (bottom panel). Between 4 and 6 plants were analyzed per treatment. ANOVA analysis at $p < 0.01$ was used to compare depth/width ratios in P treatments. Kolmogorov-Smirnov test at $p < 0.001$ was used to compare directionality distributions between the different treatments. A Local Polynomial Regression Fitting with 95% confidence interval (grey) was used to represent

the directionality distribution curve.(0^o is the direction of the gravity vector).

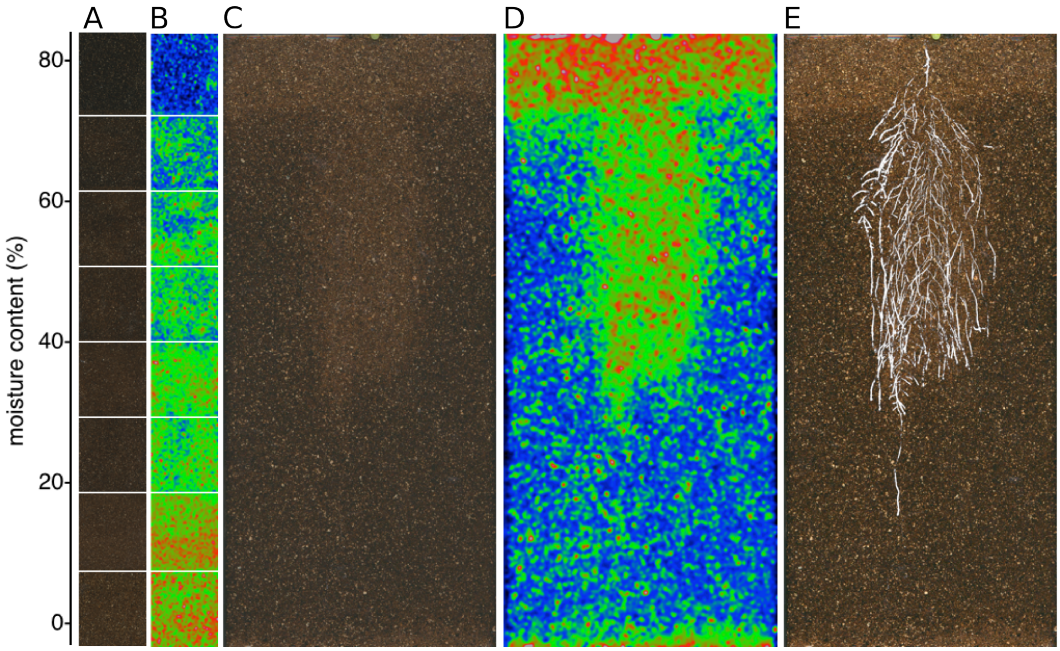

Figure 10: Soil moisture mapping in rhizotrons. A) Composite image strip made from rhizotrons prepared with different soil moisture levels. B) Differences in grey-scale intensity values were enhanced using a 16-color Look Up Table (LUT). Brightfield image of soil in rhizotron (C) and converted using 16-color LUT to enhance visualization of distribution of moisture (D) . E) Root system of a Bay-0 22 DAS and subjected to water deprivation since 13 DAS. Root system visualized using luminescence and overlaid on brightfield image of soil in (C).

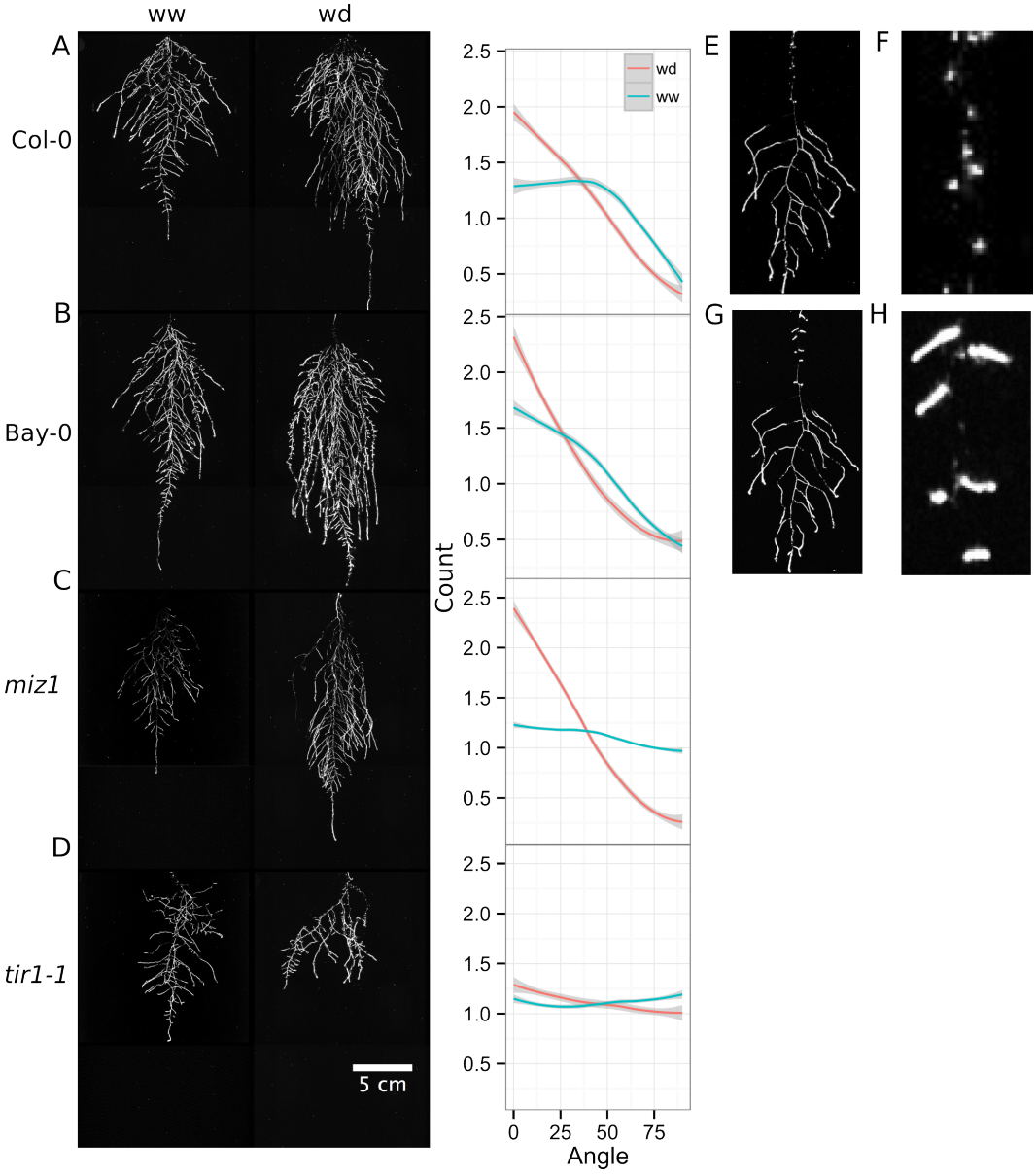

872

873 **Figure 11**: A-D) Root systems 22 DAS and exposed to water deficit 13 DAS onwards.
874 Sample images of well watered (left panels) and water deficit (right panels) root systems
875 started 13 DAS and directionality (line graphs to left of images) for (A) Col-0 (B) Bay-0
876 (C) *miz1* mutant and (D) *tir1-1* . E) Root system of a 22 DAS plant exposed to water
877 deprivation from 9 DAS onwards with magnified view of lateral root primordia (F). G) The
878 same root as in (E) 24 hours after rewatering and magnified view of lateral root primordia

(H). Kolmogorov-Smirnov test at $p < 0.001$ was used to compare directionality distributions between the different treatments and genotypes. A Local Polynomial Regression Fitting with 95% confidence interval (grey) was used to represent the directionality distribution curve.(0^o is the direction of the gravity vector).

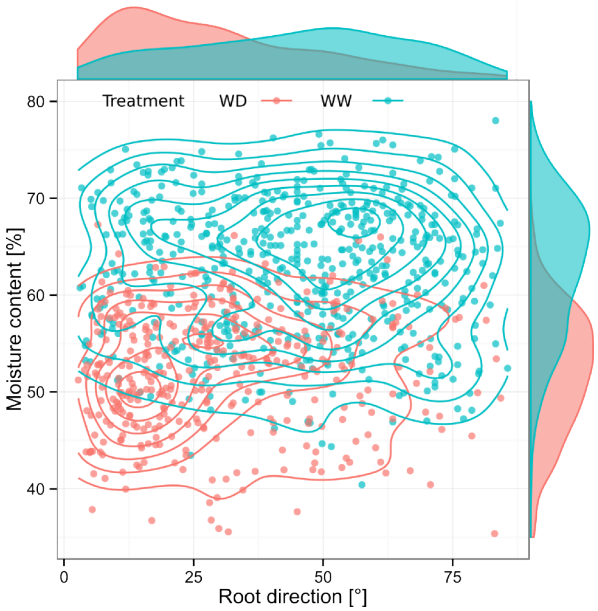

Figure 12: Relationship between local soil moisture content and root growth direction. Data quantified from the time lapse shown in Video 3. Density plots shown at periphery of graph for root direction (x-axis) and soil moisture (y-axis). (0^o is the direction of the gravity vector).

Videos

Video 1 Time lapse from 11 to 21 DAS of a Col-0 plant expressing ProUBQ10:LUC2o grown in control conditions

Video 2 24 h time lapse a Col-0 plant expressing *ProACT2:PpyRE8* (gray) and *ZAT12:LUC* (magenta) after addition of a 1 M solution of NaCl on the right side of the plant.

Video 3 Time lapse from 16 to 24 DAS of Col-0 plants expressing *ProUBQ10:LUC2o* growing in water deficient conditions (left) and control (right). Plants were sown under

895 control conditions and water deficit treatment started 11 DAS.

896 Supplementary Material

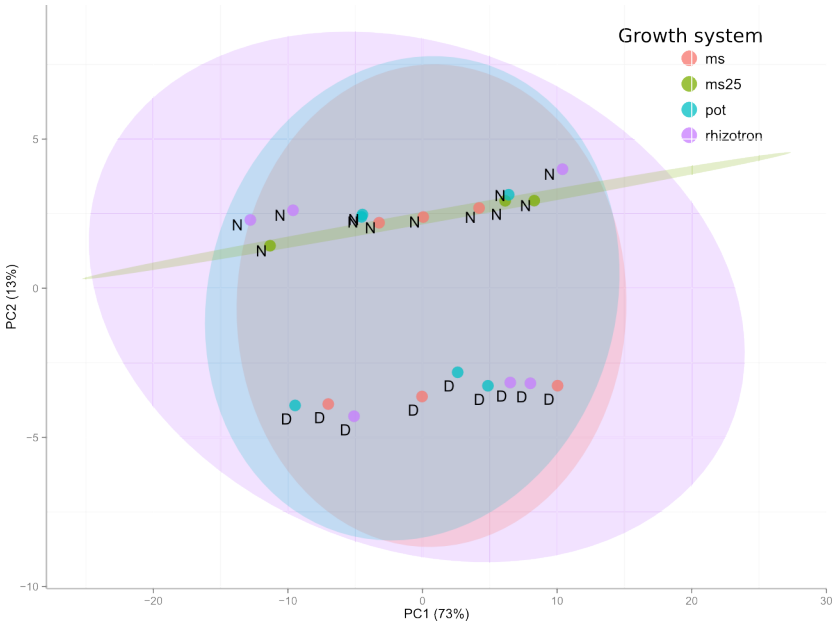

897

898 **Figure 1 Supplement 1** PCA plot of shoots of the same samples used in Figure 1. See

899 Figure 1 for more details regarding experimental conditions used.

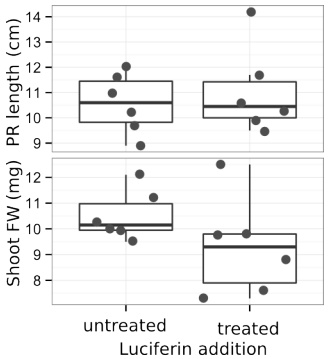

900

901 **Figure 2 Supplement 1** Effect of luciferin addition on the primary root length and shoot

902 size of 14 DAS seedlings that were either continuously exposed to 300 µM luciferin from 9

903 DAS after sowing or not.

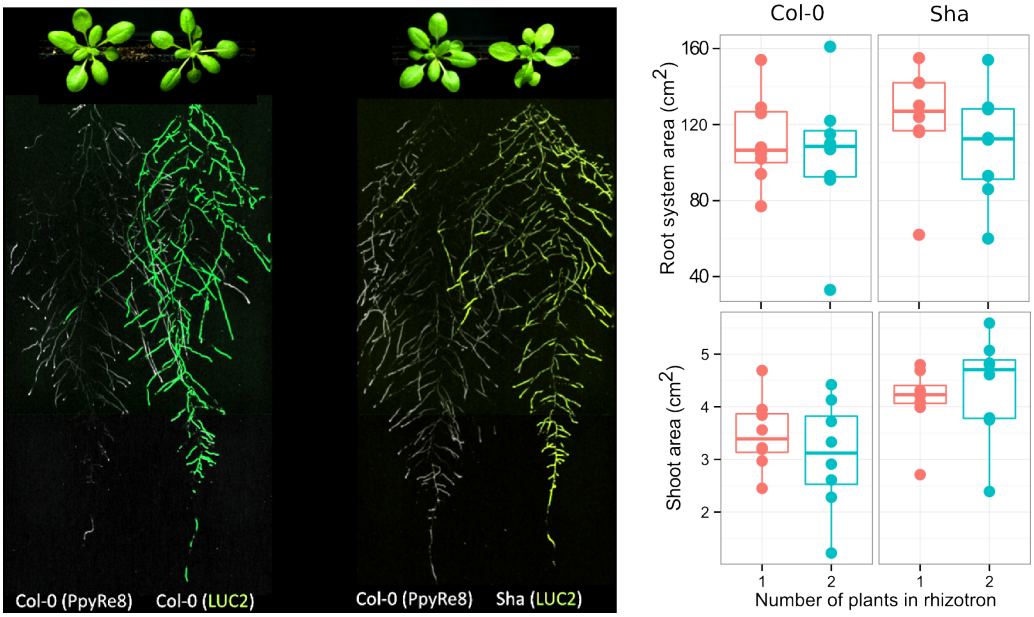

Figure 6 Supplement 1 Dual color images of 22 DAS plants growing in the same rhizotron and expressing different luciferases. A) Two Col-0 plants expressing *ProUBQ10:LUC2o* and *ProACT2:PPyRE8o* B) Col-0 plant expressing *ProACT2:PPyRE8o* and Sha plant expressing *ProUBQ10:LUC2o*.

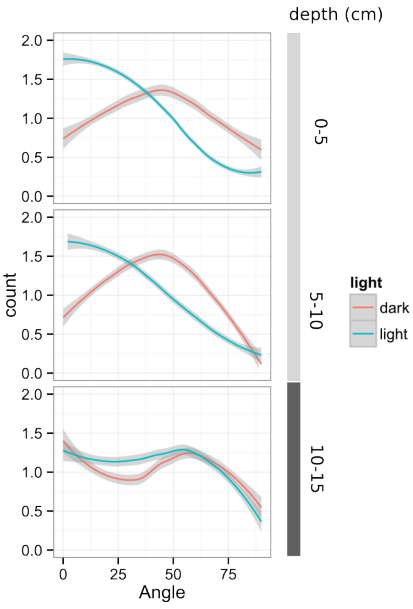

Figure 9 Supplement 1 Plots showing output of directionality analysis performed at

different depths (0-5, 5-10, 10-15 cm) in rhizotrons exposed to light or kept in the dark. (0º is the direction of the gravity vector).

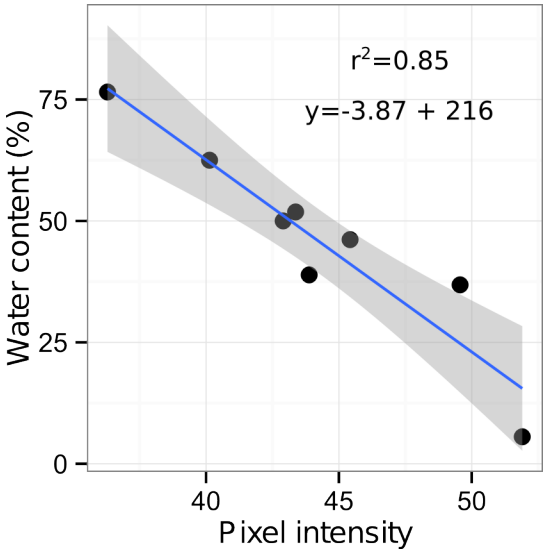

Figure 10 Supplement 1 Moisture calibration curve. Rhizotrons with different levels of moisture were prepared and scanned to obtain readings of pixel intensity. Soil from rhizotrons was then weighed, dried down in an oven at 70 ºC for 48 hours and percent water content quantified.

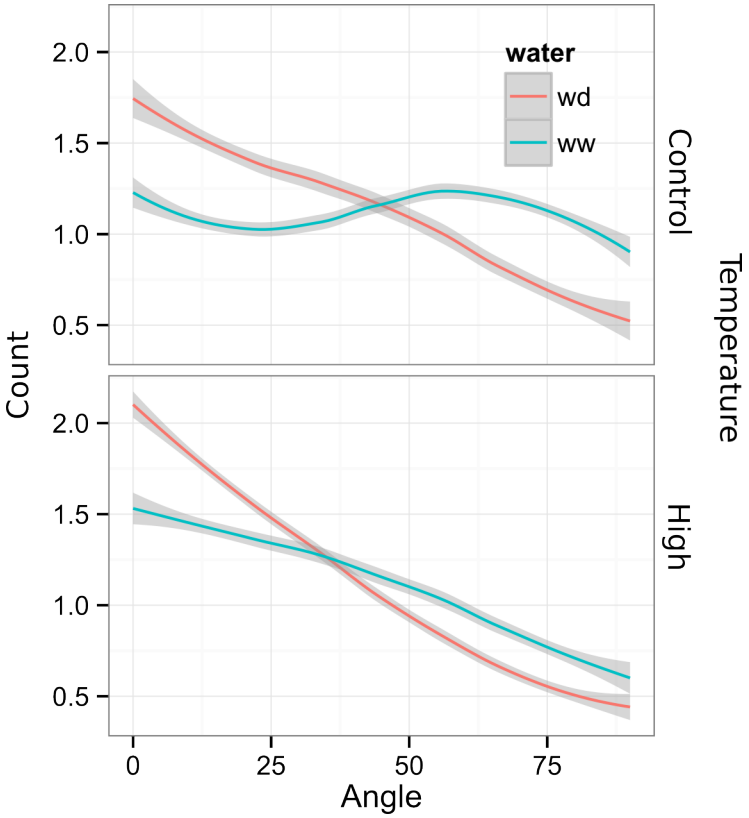

Figure 11 Supplement 1 Directionality analysis of roots of plants transferred to water deprivation conditions after 9 DAS and kept 22 ºC (control temperature) and 29 ºC (high temperature) until 22 DAS. (0º is the direction of the gravity vector).

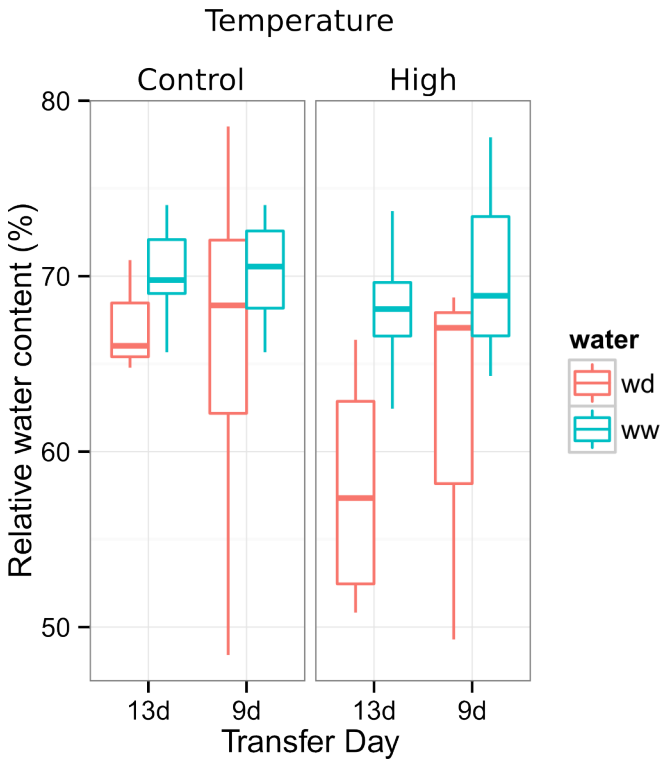

Figure 11 Supplement 2 Leaf relative water content of 23 DAS plants that were subjected to water deprivation (ww) after 9 or 13 DAS or kept under well watered (ww) conditions. At 9 DAS half of the plants were kept under control temperature condtions (22 ºC) and the other half transferred to a 29 ºC (high) chamber. n = 6-8 plants.

Supplemental Material 1

Blueprints of the holders, clear sheets and spacers needed to built the rhizotrons. Additional details are provided in the materials and methods. Files are provided in Adobe Illustrator .ai and Autocad .dxf formats.

Supplemental Material 7

Primers used in the qPCR experiment.

Supplemental Material 8

Vector maps of all the constructs used in this work.